atmosphere

MDPI

Article

Landscape Configuration Effects on Outdoor Thermal Comfort across Campus—A Case Study

Shaojie Zhang [1,2,3], Shanzhi Li [1,2], Ling Shu [1], Tieqiao Xiao [1,4,*] and Taotao Shui [5,*]

[1] School of Architecture & Urban Planning, Anhui Jianzhu University, Hefei 230022, China
[2] Prefabricated Building Research Institute of Anhui Province, Hefei 230022, China
[3] BIM Engineering Center of Anhui Province, Hefei 230022, China
[4] Anhui Academy of Territory Spacial Planning & Ecology, Hefei 230022, China
[5] School of Environment and Energy Engineering, Anhui Jianzhu University, Hefei 230022, China
* Correspondence: xtq020032@ahjzu.edu.cn (T.X.); shuitaotao@ahjzu.edu.cn (T.S.)

Abstract: As a main place for student activities on campus, outdoor spaces have positive impacts on students' physical and mental health. Namely, outdoor heat and comfort are of great significance to improve activity quality. Here, four unique outdoor spaces were studied to explore the varying effects on human thermal comfort during hot-summer and cold-winter periods. Distinct outdoor spaces (fully open, semi-open, semi-enclosed, and fully enclosed areas) from the southern campus of Anhui Jianzhu University were chosen. The PET was used as a metric for measuring thermal comfort and analyzing correlated spatiotemporal distributions. The results showed that outdoor thermal comfort was derived from multiple factors, including vegetation, underlying surface materials, building presence, and wind-heat environment. Notably, high correlations between Tmrt and thermal comfort were revealed, where such temperatures of places with trees or building shade were low; thus, PET was low. Further, Ws showed a significantly negative correlation with PET. Of the four outdoor space forms, the fully enclosed location had the lowest thermal comfort level, while the semi-enclosed spaces showed the highest level of body comfort. Therefore, semi-enclosed space (U-shaped) is recommended in campus planning and construction. Accordingly, an improved strategy was proposed based on experimental transformation for fully enclosed spaces. The thermal comfort after optimization was simulated to provide references for outdoor space thermal comfort improvement during seasonal extremes.

Keywords: campus outdoor; space form; thermal comfort; experimental transformation

Citation: Zhang, S.; Li, S.; Shu, L.; Xiao, T.; Shui, T. Landscape Configuration Effects on Outdoor Thermal Comfort across Campus—A Case Study. *Atmosphere* **2023**, *14*, 270. https://doi.org/10.3390/atmos14020270

Academic Editors: Hideki Takebayashi and Massimo Palme

Received: 13 December 2022
Revised: 24 January 2023
Accepted: 27 January 2023
Published: 29 January 2023

1. Introduction

Rapid urbanization has accelerated the process of urban heat island effects, and the resulting urban high temperatures will inherently increase energy consumption, as well as the emissions of pollutants and greenhouse gases during the summer. In turn, these actions threaten the ecological environment and sustainable development of cities, worsening urban thermal environment problems [1–3]. In a fundamental study by Lee et al., prolonged exposure to heat impacts significantly contributed to human discomfort and health problems, promoting heat-related illness [4].The use of outdoor space is highly dependent on climatic conditions. Uncomfortable outdoor spaces may hinder participation in outdoor activities and increase indoor energy consumption. Therefore, it is necessary to understand and adopt appropriate strategies to provide suitable thermal conditions for urban residents [5].

University campuses are the primary locations for students to study, live, and engage in activities; however, owing to the uncertainty and rapid transmission of COVID-19, campuses have experienced prolonged closures, severely restricting daily life and outdoor activities. Accordingly, college students have experienced frequent emotional crises [6,7]. In particular, campus outdoor spaces are an important part of the human living environment,

and have positive impacts on student health, directly affecting the quality of campus environments and human thermal comfort. Moreover, when comparing hot summers and cold winter days, higher Tas in the summer more severely limits students' outdoor activities; therefore, hot outdoor campus environment areas are worth exploring in more detail [8], yet the importance of creating a suitable microclimate environment has largely been neglected during the design, construction, and use of campuses. Further, the lack of comprehensive and systematic research on human thermal comfort across outdoor campus spaces makes it difficult to effectively guide such practices. Therefore, it is important to study outdoor microclimates and thermal comfort for improving campus environmental quality.

Thermal comfort has been defined as "the psychological state of being satisfied with the thermal environment and assessed through subjective evaluations" [9]. Accordingly, it represents an essential component of a healthy and efficient lifestyle [10]. Recently, studies addressing strategies for improving OTC have been conducted by international scholars, and they primarily include improving urban space form (building layout) [11–13], plant selection, planting methods [14–17], and choosing "cool" underlying surface materials to improve thermal environments [18,19].

The main factors affecting urban thermal comfort were the city size, street height-to-width ratio, and building orientation. Din et al. [20] confirmed that locations surrounded by buildings had lower ambient temperatures, and were the most suitable for habitation. Taleghani et al. [21] simulated courtyards in the Netherlands via ENVI-met, and concluded that the N–S direction had the shortest duration of solar radiation for hotter areas, while the E–W direction had the longest duration for courtyards, and was most suitable for cooler areas. Afshar et al. [22] proposed that a proper planting design is an important step in improving thermal comfort within urban parks. Alternatively, Milosevic et al. [23] stressed the crucial influence of tree location and canopy shape on OTC, whereas Morakinyo et al. [24] quantified the daily and seasonal microclimate behavior of various tree species with different planting designs (either individuals or in clusters), with their results indicating a possible improvement in OTC. Altunkasa [25] simulated various plant designs to improve thermal comfort at the School of Architecture, Çukurova University, Turkey. Taleghani et al. [26] also assessed thermal comfort within a university campus, and concluded that the position and orientation of high-albedo materials can significantly affect pedestrians' thermal comfort; in particular, cooler pavements maintain lower Tas, and are thus beneficial for pedestrians. Cortesao et al. [27] similarly highlighted the relevance of "cool" paving materials and vegetation in a retrofit program for urban public spaces, whereas Wang et al. [28] examined two permeable paving materials, and demonstrated that water sprinkling can boost thermal comfort above the pavement.

Relevant scholars have carried out some studies on campus OTC. Antoniadis et al. [29] conducted field microclimate measurements at two Greek universities and found that solar radiation was the main factor causing heat perception and heat stress, followed by Ws, vegetation, building materials, and building orientation. Ghaffarianhoseini et al. [30] used ENVI-met numerical simulations to evaluate thermal comfort conditions in the Kuala Lumpur campus and concluded that the spaces shaded by trees and adjacent buildings provided good thermal comfort conditions. Antoniadis et al. [31] studied the thermal environments of schoolyards, and proposed that increasing vegetation coverage could effectively improve their outdoor microclimate environment. Elsewhere, Zaki et al. [32] conducted a study on the building layout of an urban university in Malaysia, and concluded that shading of buildings directly affected outdoor Ta; thus, the outdoor thermal environment can be improved by adopting effective building morphology. Wu et al. [33] analyzed different forms of tree planting and concluded that alternative spatial arrangements of plants have different effects on the interception of short-wave radiation, leading to temperature changes. Lin studied [34] a university campus in central Taiwan and suggested that the thermal requirements of residents, as well as the characteristics of the local climate and environment, should be considered when creating shaded outdoor areas. Zhang et al. [35] developed an integrated design approach to systematically evaluate and optimize design

parameters for schools, suggesting that tree planting was the most effective strategy for a typical school in northern China.

Based on the research results, the study of microclimate and thermal comfort with ENVI-met has become an important topic in the field of landscape architecture. Most of the existing research on campus microclimate is classified by landscape elements, such as grass, squares, tree-shaded spaces, watersides, etc., and does not comprehensively consider the superposition effect caused by landscape elements and the different thermal sensations caused by the different proportions of each element. This study divides campus space into four categories, which cover different landscape elements and occupy different proportions, which can more fully illustrate the impact of landscape elements and layout on human thermal comfort. In this study conducted at the southern campus of AHJZU, PET was used as the thermal comfort evaluation index to analyze the effects of four outdoor spaces on human thermal comfort via numerical simulation techniques. Accordingly, the present study aimed to consider the effects of building heights, building modes, plants, and cushion surface material to explore the different levels of thermal comfort across each of the outdoor space forms. This information can help teachers and students more engage with these outdoor areas on campus at optimal times, as well as avoid the worst thermal comfort in time and space (e.g., in the summer, using fully enclosed area simulation renovation design to effectively improve the thermal comfort environment). This will in turn improve site utilization, in addition to saving time and cost of later renovation. Thus, this study provides a reference for improving campus thermal comfort in hot summer and cold winter areas.

The main objectives of this research were: (1) to simulate different outdoor space forms on campus (fully open, semi-open, semi-enclosed, and fully enclosed spaces) using ENVI-met, (2) to explore the varying effects of different outdoor spaces on human thermal comfort on campus using PET, and (3) to compare the spatial and temporal distribution of thermal comfort in various outdoor spaces in summer. An improvement strategy is recommended to enhance thermal comfort.

2. Research Methodology

2.1. Overview of Study Area and Measuring Points

Located in Hefei, Anhui Province of China, the southern campus of AHJZU (117°13′ E, 31°44′ N) is a typical area with hot summers and cold winters. The southern campus of AHJZU can be characterized as follows: (1) Hefei was taken as the representative hot summer and cold winter areas, and has significant climate features; (2) diverse building layouts and plant types were assessed for the study of the thermal comfort in different outdoor space forms; (3) field monitoring collected long-term data, selecting the campus as the research area, and ensuring data continuity. The architectural layout, outdoor space forms, and landscape characteristics of the AHJZU southern campus were studied and recorded by combining Google Maps, campus drawings, and field measurements. In line with existing studies on outdoor space morphology, four primary types of spaces were included here: fully open, semi-open, semi-enclosed, and fully enclosed [36]. Representative outdoor spaces were selected and analyzed in terms of building height, spatial scale, and landscape elements.

2.2. Fixed Weather Station Monitoring

Fixed meteorological observations were made using the campus IoT weather station (Figure 1), measuring parameters such as atmospheric temperature, air humidity, Ws, and direction. The 24-h meteorological data obtained on the day of measurement were used as meteorological input data for the numerical simulation. The Kestrella5500 was set 1.5 m from the ground, and automatically recorded data every 10 min [37,38]. Microclimate parameters included Ta, RH, and Ws, which are often used to analyze the outdoor thermal environment and thermal comfort [37,39]. Table 1 shows the measurement range and accuracy of this system. The numerical simulation of the outdoor microclimate on a measurement day was carried out via ENVI-met, and the field measurement data were

compared to verify software reliability. On 29 April and 13 November 2021, these two days after the start of summer and winter can represent the typical climate of summer and winter in Hefei, so these two sunny and windless days were selected for measurement from 08:00 to 18:00. Due to the limited number of experimental instruments and lower temporal resolution, Spots 1–4 were selected for field measurement on 29 April, and spots 1–6 were evaluated on 13 November. Spot distribution is shown in Figure 1.

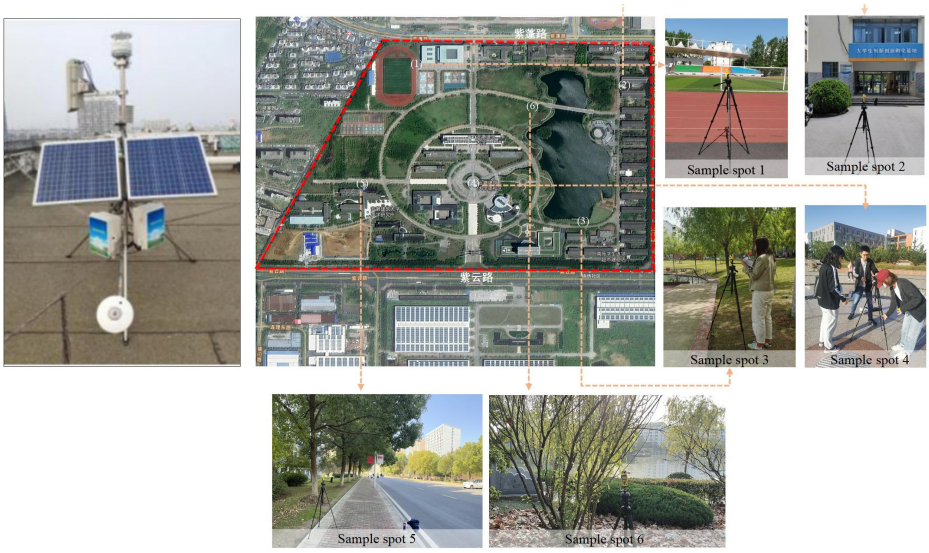

Figure 1. The campus IoT weather station and the distribution map of the measured sample spots.

Table 1. Kestrel 5500 basic parameters.

Meteorological Parameters	Measuring Range	Precision	Resolution Ratio
Ta	−30–70 °C	0.2 °C	0.1 °C
RH	0–100%	±2%	0.1
Ws	0.4–40 m/s	±3%	0.1 m/s
Wd	0–360°	±5°	1°

2.3. Analysis of Field Measurement Results

2.3.1. Analysis of Ta on 29 April and 13 November

Ta is mainly affected by solar radiation, wind, land cover conditions, and topography. Ta varies with location, height, time of day, and orientation. Figure 2 shows the hourly variation of Ta on 29 April and 13 November. The variation trend of all points is basically the same, they all rise first and then fall. The Ta reaches the peak between 14:00 and 16:00, and then drops gradually, which conforms to the Ta variation rule in one day. The Ta on 13 November drops faster than that on 29 April. On 29 April, the Ta of sample spot 3 was lower than that of other sample spots in most periods. The reason was that the underlying surface was lawn, with a large area of water in the north and willows planted in the south, which had the effect of evaporation and cooling, and the tree canopy blocked the solar radiation and the Tmrt was low. On 13 November, sample spot 5 had the lowest Ta in most periods, followed by sample spot 3.

2.3.2. Analysis of RH on 29 April and 13 November

RH refers to the amount of water vapor in the air. Water vapor enters the atmosphere through evaporation from rivers, sea, land, and plants. RH is affected by underlying surface materials, water distribution, and seasonal changes. Owing to the diurnal variation of Ta, the RH has a wide range. Usually, the RG is the lowest when the Ta is the highest at noon and the RH is higher when the Ta is lower. Figure 3 shows the hourly variation of the

measured RH on 29 April and 13 November. It can be seen that the variation trend of RH is opposite to that of Ta.

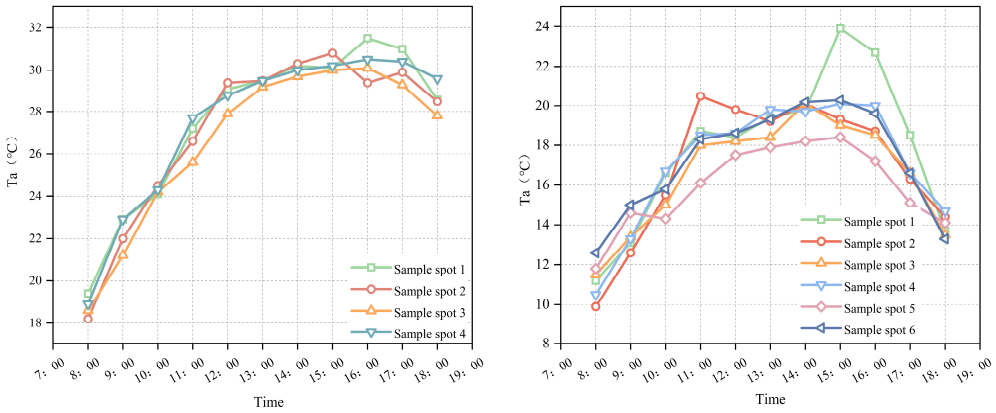

Figure 2. Measured Ta change map on 29 April and 13 November.

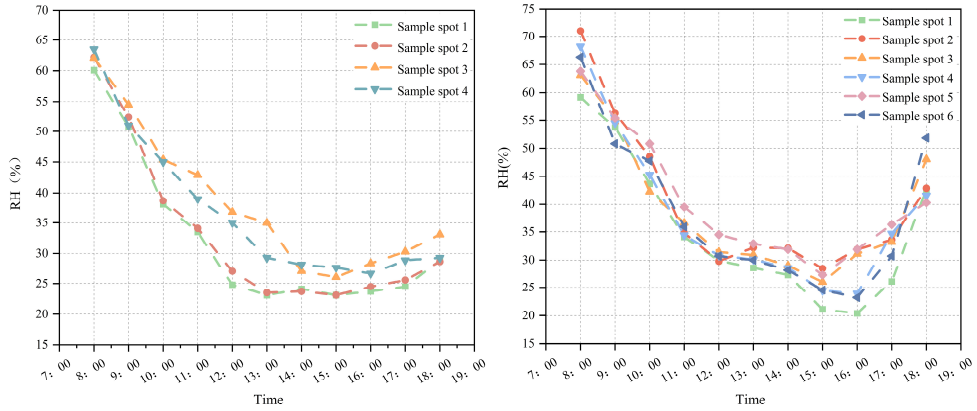

Figure 3. Measured RH change map on 29 April and 13 November.

2.4. ENVI-met Validation Model Building and Analysis

ENVI-met is the popular numerical simulation software in microclimate research and has also been used to designed to simulate the interaction of buildings, vegetation, and the underlying surface with the regional atmosphere to calculate human thermal comfort indices [40]. Numerous studies have been conducted using ENVI-met in parks, residential areas, and other locations. Sun et al. [41] evaluated the thermal comfort of a long belt-shaped park (about 9 km) in Beijing through ENVI-met numerical simulation; there, the outcome provided suggestions for urban landscape planners to improve thermal comfort. Similarly, Mahmoud and Abdallah [42] used the ENVI-met model *v*.5.0.0 to set up different shading strategies aimed at improving OTC for students. Elsewhere, Rui [43] conducted a simulation based on the morphology and green layout of Nanjing, and the microclimate study was evaluated using ENVI-met across residential areas. Yang [44] verified the effects of different greening patterns on OTC in residential districts, whereas Yang et al. [45] investigated the influence of various street orientations, height-to-width ratios (H/W), and vegetation on OTC in urban streets using ENVI-met. Narimani et al. [46] used an ENVI-met simulation to enhance the thermal comfort of street canopies, while Karimi [47] examined the determinant factors of the thermal environment and strategies related to albedo and greenery in a medium-scale park using ENVI-met software. Lastly, Chan et al. [48] used ENVI-met to formulate a simulation model for analyzing OTC under various microclimatic conditions in parks and surrounding buildings.

2.4.1. ENVI-met Model Building

The satellite base map was converted into BMP format, and imported into ENVI-met; thus, the simulation model was built in ENVI-met based on the satellite base map. As stated above, all required meteorological data were obtained from the school's IoT weather station. The site model map was built in ENVI-met, and the simulation was conducted using the weather station data from 29 April and 13 November as its basic conditions (Tables 2 and 3) [49].

Table 2. Boundary conditions of the simulation process by ENVI-met model.

Boundary Conditions of the Simulation Process by ENVI-met Model	
Location	Hefei (117°13′ E, 31°44′ N)
Climate	Humid subtropical climate (Cfa)
Simulation date	29 April and 13 November 2021
Simulation time	From 08:00 to 19:00
Model dimensions	x-Grids: 229; y-Grids: 150; z-Grids: 40
Grid cell	dx = 5 dy = 5 dz = 4
Vegetation	Simple plants and 3D plants
Materials	Table 3
PET index calculation	BIO-met process
Results visualization	Leonardo visualization tool

Table 3. Underlying surface material and albedo.

Physical Properties	Soil Materials						
	Loamy Soil	Dark Granit Pavement	Asphalt Road with Red Coating	Asphalt Road	Concrete Pavement Gray	Granit Shinning	Brick Road
Albedo	0.0	0.3	0.5	0.2	0.5	0.8	0.3
Emissivity	0.98	0.9	0.9	0.9	0.9	0.9	0.9

2.4.2. ENVI-met Software Reliability Validation

In many previous studies, verification of ENVI-met results was done by comparing the results of simulations and field measurements, the results of which showed that the software simulated environmental conditions with appropriate accuracy. In their literature review on numerical simulation studies of OTC, Lam et al. [50] found that Ta was the most important validation parameter, followed by Tmrt, and RH. Yang et al. [44] examined the correlation between measured and simulated Ta and RH, and the results show that there is a strong correlation between the measured and simulated values. Muller et al. [51] evaluated the model performance by comparing the values of Ta and RH field measurements and simulations, and they observed that the model accurately reproduced the observations. Farhadi et al. [52] compared Ta measurements and simulated values in the study, and the results proved that the ENVI-met simulation results had an acceptable level of accuracy. Notably, these parameters were mainly validated by the coefficient of determination (R^2), root mean square error (RMSE), and mean error (ME). When conducting numerical simulations using ENVI-met, Salata et al. [53] employed the following evaluation metrics: R^2, RMSE, and the consistency index (*d*). The author pointed out that ENVI-met performed accurately and could be used to predict the microclimate of a site when R^2 approached 1, RMSE approached 0, and *d* approached 1.

As the measuring instrument used in this study could not monitor Tmrt, the Ta and RH were chosen as validation parameters, and correlation metrics were evaluated using the R^2, RMSE, and *d* as validation metrics for both field and simulated measurements.

2.4.3. Analysis of the Measured Data and the Simulated Data

The validation showed that on 29 April, the Ta R^2 ranged from 0.937 °C to 0.969 °C, while the RMSE ranged from 1.078 °C to 2.715 °C, and *d* ranged from 0.828 °C to 0.974 °C,

approaching 1 °C; thus, each indicated that ENVI-met could predict variable indicators relatively well. Furthermore, the RH R^2 ranged from 0.843 to 0.99, the RMSE ranged from 2.11% to 10.06%, and *d* ranged from 0.843 to 0.990, whereas the simulation results represented the hourly trends of the measured values. On 13 November, the number of measured and simulated sample points increased, with Ta R^2 ranging from 0.66 °C to 0.78 °C, RMSE ranging 1.26–2.72 °C, and *d* ranging 0.74–0.89 °C. Additionally, RH R^2 ranged 0.68–0.88, RMSE ranged 4–9.7%, and *d* ranged 0.79–0.92, notably all within acceptable limits (Figures 4 and 5 and Tables 4 and 5).

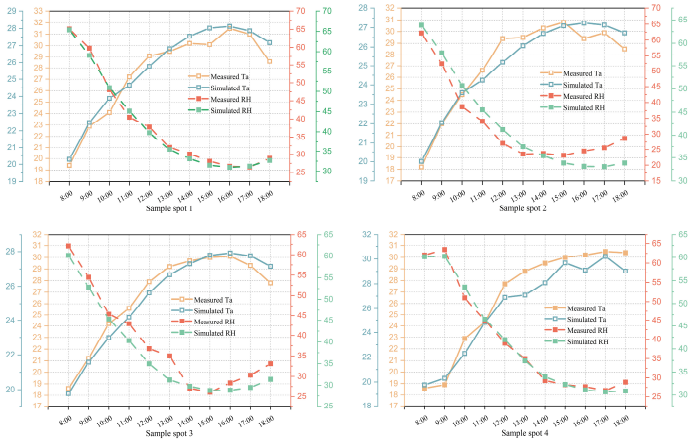

Figure 4. Comparison between the measurement and simulated Ta and RH of the sample spots on 29 April.

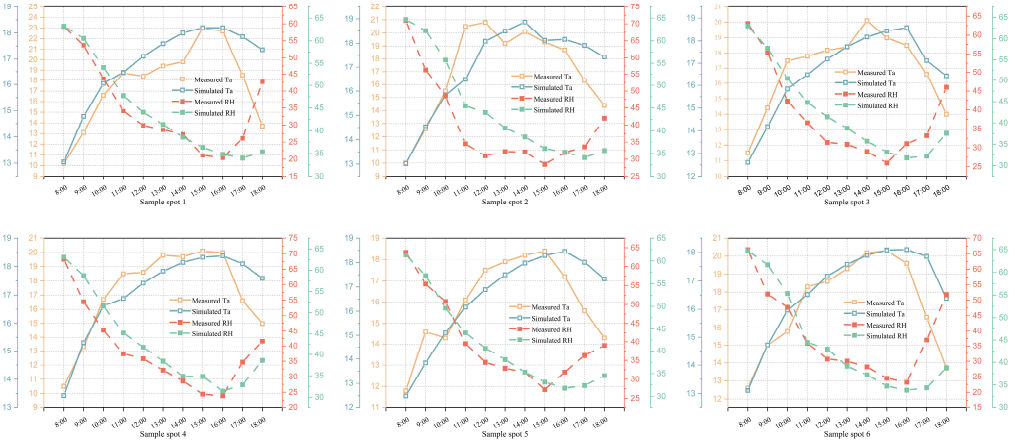

Figure 5. Comparison between the measurement and simulated Ta and RH of the sample spots on 13 November.

Table 4. Quantitative evaluation results of model accuracy of ENVI-met various sample spots on 29 April.

Sample Spot	Variable	R^2	RMSE	*d*
Sample spot 1	Ta	0.96	2.35	0.84
	RH	0.99	3.33%	0.98
Sample spot 2	Ta	0.94	2.72	0.83
	RH	0.93	10.06%	0.84
Sample spot 3	Ta	0.97	1.78	0.93
	RH	0.97	2.11%	0.99
Sample spot 4	Ta	0.97	1.08	0.97
	RH	0.99	3.20%	0.98

Table 5. Quantitative evaluation results of model accuracy of ENVI-met various sample spots on 13 November.

Sample Spot	Variable	R^2	RMSE	*d*
Sample spot 1	Ta	0.73	2.72	0.74
	RH	0.75	9.70%	0.79
Sample spot 2	Ta	0.69	2.17	0.82
	RH	0.77	7.63%	0.90
Sample spot 3	Ta	0.78	1.26	0.91
	RH	0.78	6.53%	0.91
Sample spot 4	Ta	0.78	1.85	0.82
	RH	0.83	6.30%	0.92
Sample spot 5	Ta	0.66	1.31	0.89
	RH	0.88	4.00%	0.96
Sample spot 6	Ta	0.71	1.64	0.86
	RH	0.68	9.23%	0.85

In summary, the errors in Ta and RH at each site were acceptable, although the ENVI-met showed better performance in the summer than in winter (*d* was closer to 1) [54,55]. Thus, it was concluded that the ENVI-met model can provide a reasonable estimate of the measured data in this study, and accurately simulate the microclimate of the university campus in Hefei, in addition, to accurately reflecting the main spatiotemporal distribution characteristics.

2.5. Simulation Date

June was selected as the summer month for assessing microclimate and thermal comfort. At least three consecutive typical meteorological days were selected to calculate the summer campus microclimate values. These days saw no rainfall, and their meteorological indices, such as Ta, RH, wind direction, and Ws, were all similar to the summer meteorological index averages [56], which were deemed representative of the general climate characteristics for June. Through the screening of meteorological data, 22 June was selected as the summer study date for simulation. On that day, the maximum and minimum Tas were 33 °C and 20 °C, respectively, whereas the Ws was approximately 3 $m \cdot s^{-1}$, with prevailing winds coming from the east.

Based on the campus IoT weather station data of the AHJZU southern campus on 22 June, the initial meteorological parameters, hourly Ta, and RH data were input as the simulation base conditions. To take into account the experimental efficiency and accuracy of the results, the simulation was set to a simple forced mode, with an initial simulation time starting at 05:00, and lasting 20 h. The first 3 h were the experimental warm-up stage.

2.6. Characteristics of the Four Spaces

Four types of outdoor spaces (fully open, semi-open, semi-enclosed, and fully enclosed) were simulated, and the PET values were calculated using ENVI-met. Four time points were selected: 09:00, 12:00, 15:00, and 18:00. Pedestrian-level PET values at each time point were exported to compare the spatiotemporal distribution of thermal comfort at different time points. The proportion of the study area occupied by PET values at each level was plotted.

Stewart and Oke [57] proposed the local climate zones (LCZ) theory to quantify local-scale spatial morphology characteristics to parameterized type units and Liu et al. [8] introduced this theory to campus, which included six spatial morphology features: sky visual factor (SVF), aspect ratio (AR), roughness unit height (HRE), building surface fraction (BSF), permeable surface fraction (PSF), and permeable face fraction (ISF). Among these, SVF, AR, and HRE reflect the geometric layout, whereas BSF, ISF, and PSF describe the land overlying pattern. Thus, these six parameters can represent the spatial morphological fea-

tures of the university campus. The detailed acquisition and calculation of the parameters were performed as follows (Table 6).

Table 6. Acquisition and calculation of the parameters.

Parameters	Collection Methods	Calculation Formula	Explanation
SVF	Calculation through SAGA-GIS	$SVFcanyon = \cos\left(\tan^{-1}\left(\frac{2*H_{can-bu}}{W_{can-str}}\right)\right)$	SVF_{canyon} is the SVF calculated at the middle of the street canyon; H_{can-bu} is the building height of the street canyon, m; $W_{can-str}$ is the width of the street canyon, m;
AR	Building a 3D model combined with field investigation	$AR = \frac{H}{W}$	H is the height of the zone, m; W is the width of the street canyon in the zone, m;
HRE/m	Building a 3D model combined with field investigation	$HRE = \frac{\sum_{i=1}^{n} h_i}{n}$	h_i is the height of the building in a zone, m; n is the number of buildings in the zone
BSF/%	Building infographic through Google Earth satellite imagery and mapping software	$BSF = \frac{S_b}{S_{total}}$	S_b is the base area of the building in the zone, m; S_{total} is the total area of the zone
PSF/%	Collecting through Google Earth satellite imagery	$PSF = \frac{S_p}{S_{total}}$	S_p is the permeable area in the zone (bare soil, green plant, water boby, etc.), m^2; S_{total} is the total area of the zone, m^2
ISF/%	Collecting through Google Earth satellite imagery	$ISF = \frac{S_i}{S_{total}}$	S_i is the impermeable area in the zone (asphalt pavement, bare rock, etc.), m^2; S_{total} is the total area of the zone, m^2

The four spatial types are enclosed by different building patterns as part of the spatial boundary; therefore, BSF was not considered in this study. The remaining five parameters for each study site are shown below (Figure 6).

2.7. OTC Calculation

Several indices that integrate thermal factors based on the energy balance of the human body were employed to assess OTC. The common indices are PET, UTCI, SET *, and UTCI. Among them, PET is the most widely used comprehensive parameter [10], which is consistent with the findings of Kumar. Huang et al. [58] studied the OTC of a university campus in Mianyang, Sichuan during a hot summer and cold winter, ultimately determining the seasonal PET. The study showed that 90% of people had PET acceptance values <35.6 °C in summer, and >20.2 °C in winter. When PET increased, the probability of "using an umbrella", "dressing", and "going to shade" increased by 22.6%, 4.9%, and 16.6%, respectively, whereas the probability of "staying in sunlight" decreased by 17.5%. Liu et al. [8] studied nine experimental sites across a Shanghai university, and found that under hot and humid climate conditions, the thermoneutral PET range of college students inhabiting outdoor spaces was 29.16–32.04 °C, which is highly similar to those in other regions of China. PET proved to be more suitable for the study of thermal comfort in the warm season in China [59].

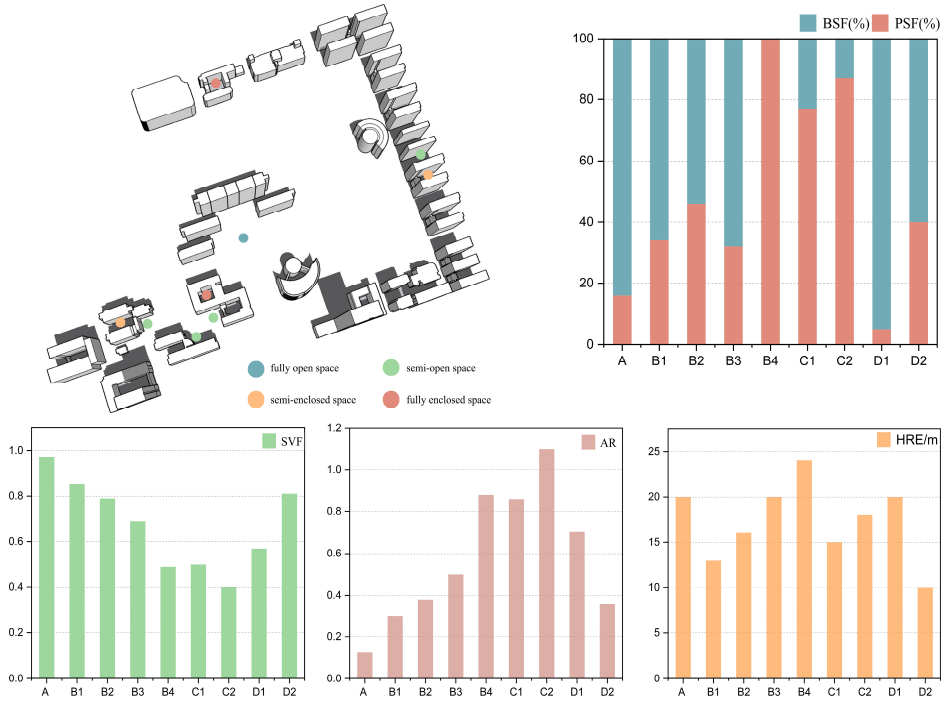

Figure 6. Local zone divisions within the campus in AHJZU and the distribution chart of spatial morphology characteristic parameters in each local zone.

Here, the PET was calculated to predict human thermal perception. Because the thermal comfort index is influenced by geographical location and climate, thermal perceptions were divided into nine grades according to different climate zones, although the difference in human thermal perception in different climate zones is relatively small [60]. Both Hefei and Changsha belonged to the *Cfa* climate zone [61]; therefore, Liu's [62] study on thermal comfort in Changsha was referenced, and the resulting modified PET range was adopted as the OTC evaluation standard for Hefei (Table 7). Outdoor neutral temperature reflects human requirements for thermal comfort in outdoor environments, which is defined as outdoor temperature causing people feel neutral (neither cold nor hot). In general, neutral temperature is a comfortable thermal condition and can be accepted by most people. In summer, people are more adapted to neutral or warm environments, and when the outdoor environment is hot or very hot, people are poorly adapted to the microclimate.

Table 7. PET value level range division.

Thermal Sensation	Very Cold	Cold	Cool	A Bit Cool	Neutral	Slightly Warm	Warm	Hot	Very Hot
PET (°C)	<−8	−8–−1	−1–7	7–15	15–22	22–30	30–38	38–46	>46

3. Results and Discussion

3.1. Spatiotemporal Distribution of Thermal Comfort in Fully Open Space

A fully open space (A) was represented by a round square south of the main teaching building (Figure 7). It is a stilt building approximately 32 m high, with five-story buildings existing along its southwest and southeast sides. The central area is mainly paved with sesame gray granite, which maintains high reflectivity, while the square is surrounded by *Cinnamomum camphora (Linn) Presl.*, *Osmanthus fragrans (Thunb.) Lour*, *Loropetalum chinense var. rubrum* and lawns. The central area is planted with *Malus micromalus* and *Pyracantha fortuneana (Maxim.) Li*, while the southwest side is planted with *Osmanthus fragrans (Thunb.) Lour*, *Cerasus* sp. and *Photinia x fraseri Dress*.

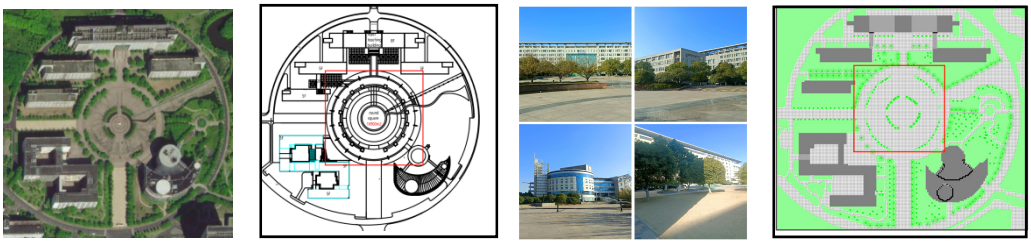

Figure 7. Site information of fully open space.

At 09:00, owing to the impacts of Ws and plants, a lower PET value was found in the area shaded by camphor trees, because not only is the solar radiation being weakened by tree canopies, but a high Ws exists at the corner of the building. The highest value was found in the southwest corner of the site, in the area adjacent to buildings, producing a thermal sensation between "slightly warm" and "very hot". At 12:00, as the solar altitude angle increased, and the shadows of the buildings and plants decreased, the PET value gradually increased as well, with most of the square having a PET value of 44–45 °C, indicating a thermal sensation of "hot". The lowest PET value was measured under the *Osmanthus fragrans (Thunb.) Lour* in the square (yellow area in Table 6), where the Ta and Tmrt were both low, as the lawn underneath this vegetation supplied cooling and humidifying effects, while the long-wave radiation at the lawn was weaker than at the paved area. At 15:00, the overall PET values in the square increased again, and the lowest PET value was measured in the tree shade, while the highest PET value was found at the entrance of the library (≤62 °C, extremely poor thermal comfort environment). At 18:00, the PET value in the square area ranged from 28 °C to 40 °C, and owing to the influences of the buildings along the northwest side, the PET values were the lowest in the northwest area of the square, and highest in the southeast area of the square (approximately 39 °C, "hot" thermal sensation) (Figure 8).

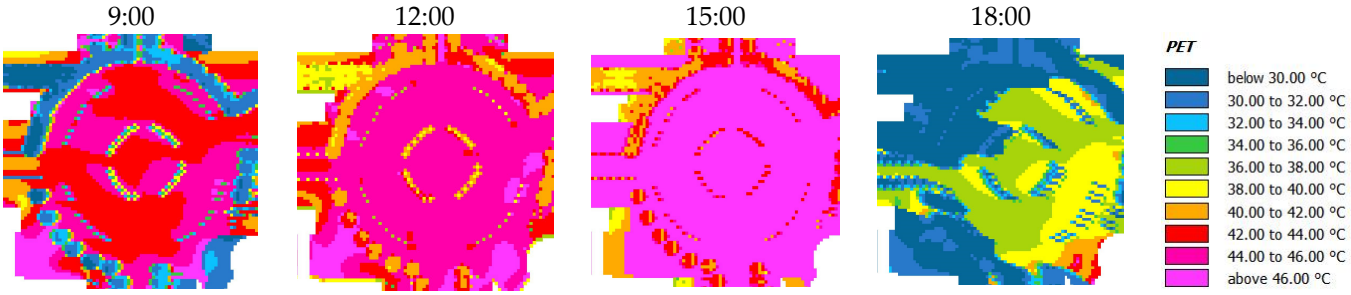

Figure 8. The spatiotemporal distribution of the PET in a fully open space.

3.2. Spatiotemporal Distribution of Thermal Comfort in Semi-Open Space

Semi-open spaces are mainly L-shaped or parallel to each other, and most are located at the entrance plaza of academic buildings, or in the courtyard between dormitory buildings. Four semi-open spaces on the campus were selected for the numerical simulation and study, three of which were L-shaped and located at the entrances of academic buildings, and one of which was an area between two dorms.

B1: The science and chemistry laboratory building complex includes 4- and 5-story buildings. The entrance plaza is located at the southeastern corner of the building, as shown at point 1. Landscape elements include flamed surface plaza tiles, trees, and low shrubs. *Cinnamomum camphora (Linn) Presl* and *Prunus Cerasifera Ehrhar f. atropurpurea (Jacq.) Rehd* were the main trees, while *Buxus sinica (Rehd. et Wils.) Cheng* and *Loropetalum chinense var. rubrum* were the main shrubs.

B2: The mechanical and electrical building complex includes 2- and 5-story buildings. The entrance plaza is located at the northeast corner of the building complex, as shown in point 2. The landscape elements include concrete red brick, trees, low shrubs, lawns,

Cinnamomum camphora (Linn) Presl, *Ginkgo biloba* L., *Osmanthus fragrans (Thunb.) Lour*, and shrubs, such as *Platycladus orientalis*, *Buxus sinica (Rehd. et Wils.) Cheng*, and *Photinia x fraseri Dress*.

B3: The Yifu Building is 5 stories tall, and the entrance plaza is located at its southwest corner (point 3). The landscape elements are stone, trees, low shrubs, and lawns, such as *Sapindus*, *Ginkgo biloba* L., *Cinnamomum camphora (Linn) Presl*, *Platanus acerifolia* and *Cerasus* sp., while the shrubs are primarily *Buxus sinica (Rehd. et Wils.) Cheng*. The lawn area is relatively large (Figure 9).

Figure 9. Site information of B1, B2, and B3 spaces.

B4: The semi-open space parallel to the two buildings was mostly located in the semi-open dormitory area enclosed by dormitory buildings 10 and 11. It has a length of ~60 m, and a width of ~27 m, without hard pavement. The main landscape elements are lawns and trees, mainly including *Pinus*, *Sapium sebiferum* (L.) *Roxb*, *Prunus Cerasifera Ehrhar f. atropurpurea (Jacq.) Rehd*, and *Photinia x fraseri Dress* (Figure 10).

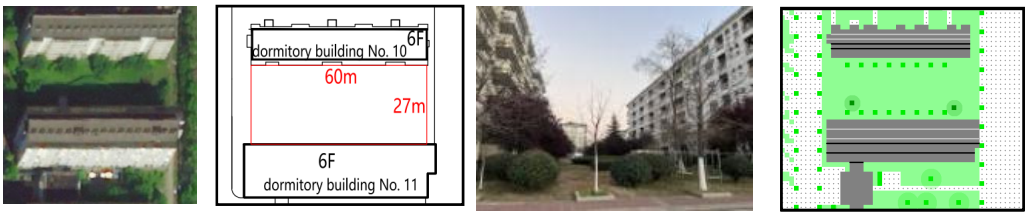

Figure 10. Site information of B4 space.

The thermal comfort of semi-open spaces at pedestrian heights across the four time periods were compared and analyzed. As shown in Figure 11 (where the white area represents the buildings), PET distribution at different time points varied owing to the differences in the positional relation between the semi-open space, the adjacent building, plant planting, and paving.

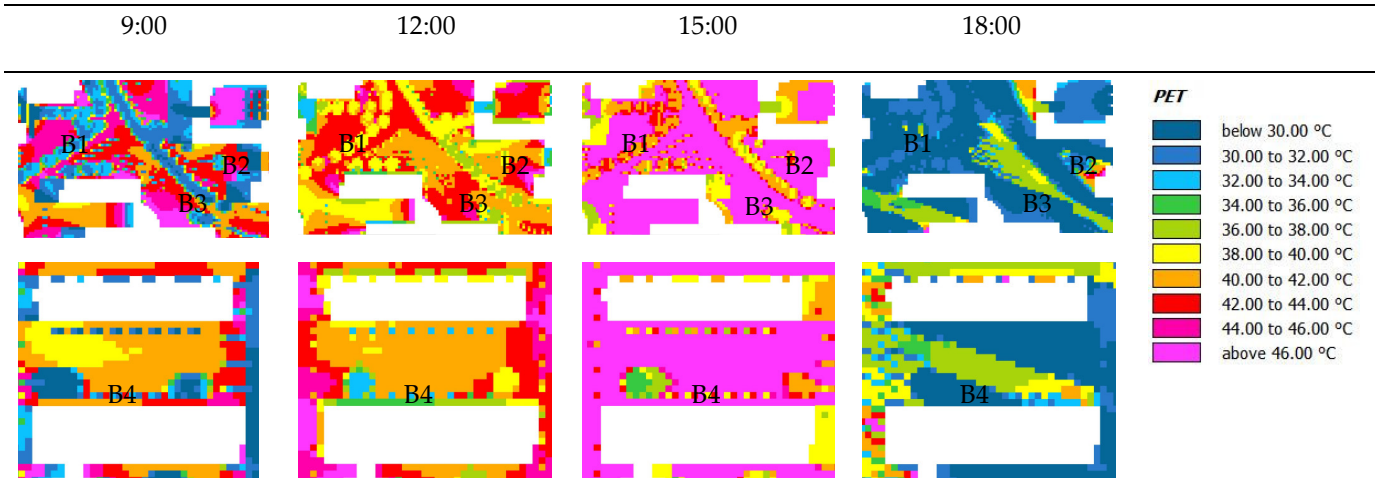

Figure 11. The spatiotemporal distribution of the PET in the semi-open space.

At 09:00, the highest PET values were found in a small area to the east of building B1, as it was perpendicular to the prevailing wind direction, whereas along the east side of the building, a high-pressure area formed against the wind, reducing its speed, and motionless people would not feel the wind. Area B1 is mainly covered with hard paving materials and showed higher Tmrt and PET values. The PET values were lower in area B2, which was shaded by a connecting corridor of buildings and trees. Area B3 was not shaded by buildings or trees, and had higher PET values, along with the worst overall thermal comfort. Area B4 is underlain by lawns, while the site is also planted with trees. Further, the Ws between the two buildings is high, resulting in a lower overall PET value. At 12:00, the PET values under the trees were the lowest, whereas most places in areas B1, B2, and B3 had PET values between 44 and 47 °C. B2 and B3 had the highest PET values in two areas adjacent to the buildings that were located on the eastern windward side of a B2, and west windward side of B3, where a high-pressure area was formed, reducing its speed. Therefore, the Ws in these two areas were low, and the resulting PET values were the highest. At that time, the underlying surface of area B4 was lawns, while shrubs and trees were planted, producing strong evaporative cooling effects. The overall Tmrt was the lowest here, and the thermal comfort environment in area B4 was improved. At 15:00, the PET value reached its peak, as Tas and solar radiation increased. The lowest values of PET were distributed in the shadows of B1 and B2 squares, as well as in the shadows of B1, B2, and B4 trees. The highest PET values were also observed in areas with low Ws, such as the leeward sides of B2, B3, and B4. At 18:00 as the sun set to the northwest, the solar elevation angle decreased, and PET values gradually decreased as well. PET values were below 30 °C in most areas, and the overall thermal comfort environment was good (Figure 11).

3.3. Spatiotemporal Distribution of Thermal Comfort in Semi-Enclosed Spaces

Semi-enclosed spaces(U-shaped) are enclosed on three sides, their connections to the outside vary with the orientations of courtyards, and they often have a stronger sense of enclosure and centrality than semi-open spaces. These usually refer to the courtyard spaces of a building. A semi-enclosed area between the courtyard of a science and chemistry laboratory building, and a dormitory building were chosen for the thermal comfort study, and its openings were oriented in opposite directions.

C1: The courtyard of the Science and Chemistry Building is a semi-enclosed space in the teaching building area. It is about 54.5 m long and 23 m wide. The height of the building on the north and south sides is approximately 20 m, with a 4-story building on the east side, along with a 5-story corridor. The courtyard is rectangular, and the main landscape elements are trees, globe-shaped shrubs, lawns, and pavement. The trees are planted freely, such as *Michelia figo (Lour.) Spreng*, *Osmanthus fragrans (Thunb.) Lour*, *Cinnamomum camphora (Linn) Presl* and *Photinia x fraseri Dress*. The hard paving used square flamed surface tiles (Figure 12).

Figure 12. Site information of C1 space.

C2: The courtyard between dormitory buildings No. 11 and No. 12 is also semi-enclosed. Located on the east side of the building, it is ~42 m long and 21 m wide. The buildings on the north and south sides are approximately 20 m high, and there is a two-story building along the west side. The main landscape elements are trees and lawns, with

the former including *Cinnamomum camphora (Linn) Presl*, *Osmanthus fragrans (Thunb.) Lour* and *Photinia x fraseri Dress*, which were planted freely (Figure 13).

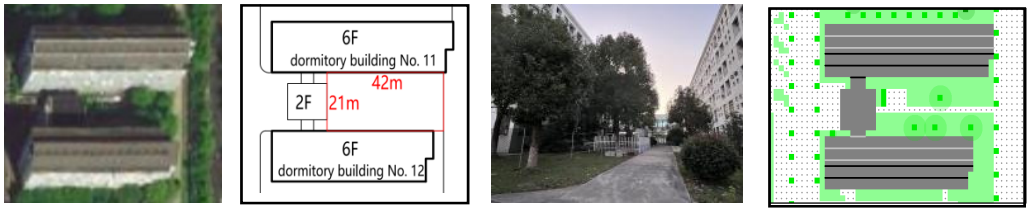

Figure 13. Site information of C2 space.

Figure 14 shows that the spatiotemporal distributions of the thermal comfort in C1 and C2 were similar. At 09:00, the lowest PET values in area C1 were found in the left corridor and under the shade of trees, whereas for area C2, the lowest values were observed in the tree shade. At 12:00, the PET values under the trees in C1 and C2 were low, and the thermal sensation was "warm". Further, the PET values in the lawn were also low. The highest PET value areas were mostly those covered with hard paving materials, with PET values ranging from 45 °C to 47 °C. At 15:00, the overall PET values were high in the study areas, mainly behind buildings and plants with low wind velocities. In C1, the lowest PET values were found on the north side of the site, where shrubs and trees were planted with low Tmrt. Comparatively, the PET values in the building and tree shade of C2 were low (~35 °C). At 18:00, all PET values were below 32 °C in area C2, while they remained high in parts of C1's central area (38–41 °C).

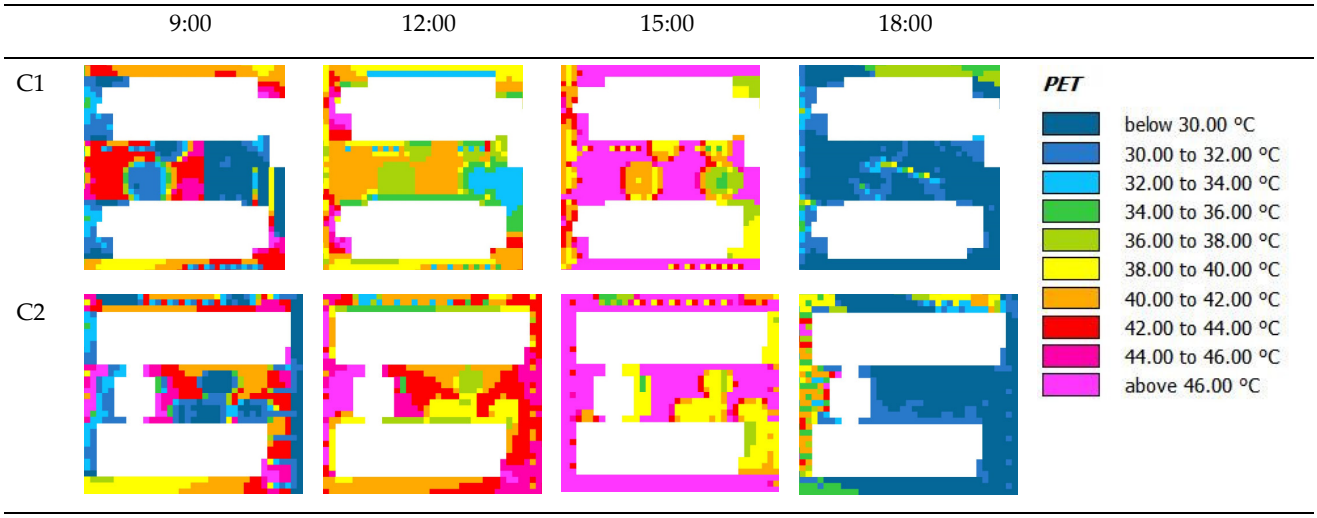

Figure 14. Spatiotemporal distribution of PET in the semi-enclosed space.

3.4. Spatiotemporal Distribution of Thermal Comfort in Fully Enclosed Spaces

Fully enclosed spaces are enclosed by buildings on four sides, and the sense of centrality, closure, and privacy of the courtyard is very strong. The courtyards of the Logistics Complex (D1) and the Yifu Building (D2) were selected for this study. The sites are both courtyard spaces within buildings, but the building heights, as well as their forms of enclosure differ.

D1: In the Yifu teaching building area, the courtyard on the northwestern side is a fully enclosed space (Figure 15). The courtyard is enclosed by buildings on all four sides: the buildings on the south, north, and west sides of the courtyard are approximately 20 m high, while the building to the west is partially elevated, and the building to the east is approximately 4 m high. The courtyard is rectangular, and about 30.5 m long and 28 m wide. The main landscape element is granite pavement, and the site was relatively spacious.

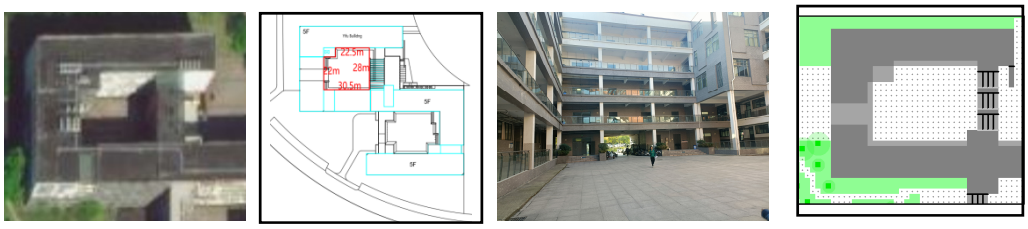

Figure 15. Site information of D1 space.

D2: The courtyard of the logistics complex in the living area is shown in Figure 16. The buildings in the site are mainly 2–3 stories, and the space formed by the two buildings is less enclosed than the courtyard of the D1. The center of the courtyard is a small, hard-paved recreational square, surrounded by lawns, *Cinnamomum camphora (Linn) Presl*, *Diospyros kaki Thunb*, and *Osmanthus fragrans (Thunb.) Lour* which are planted to the north side of the site, while shrubs are planted along the east and south sides.

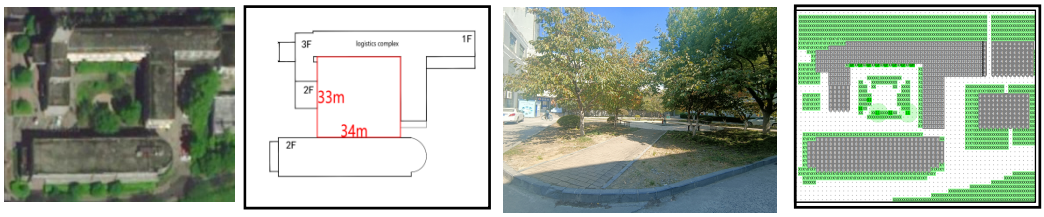

Figure 16. Site information of D2 space.

3.4.1. Spatiotemporal Distribution of Thermal Comfort

At 09:00, the lowest PET values in both D1 and D2 were found in the areas with the lowest Tmrt, such as the shadows on the west side of the building. Additionally, the high connecting corridor on the right side of D2 created a large area of shadows, and the ground floor was ventilated, resulting in a lower Tmrt than D1; thus lower PET values on the right side of D2 were created than in D1. The maximum PET values were also found in areas with low Ws and direct sunlight, such as the northwest and northeast corners of D1, and the north and south sides of D2 (rose red indicates the highest PET value). At 12:00, the minimum PET value in the D2 courtyard was found in the overhead space of the building's ground floor, whereas the minimum value in D1 was found in the shadow overlap of the north building and osmanthus trees. The maximum PET values were found at the corner of the building on the north side of D1, as well as in areas with low Ws to the north and south sides of the courtyard. At 15:00, the PET values in the shades of the buildings on the west side areas of D1 and D2 were the lowest, and the PET value in the shadow of D2 was lower than that in D1 because of the larger shaded area created by the buildings on the west side of D2. The highest PET values were also found in areas with direct sunlight and low Ws. At 18:00, the PET values of most areas of D1 and D2 ranged from 30 °C to 32 °C, and the thermal sensation was "warm". The southwest side of D1 was exposed to direct sunlight and had a high Tmrt, thus, the PET value was high (37–39 °C), but the Ws on the south side was lower than that to the west, so its PET value was higher as well (Figure 17).

3.4.2. Percentage of Thermal Comfort Grade at 9:00

At 9:00, thermal comfort in fully open spaces was graded as "slightly warm", "warm", "hot, and "very hot". The PET value in most areas fell between 38 °C and 46 °C, providing a "hot" thermal sensation. In the semi-open space, B2 had the highest proportion of "slightly warm" areas (18.4%), followed by B4 (12.6%); B4 had the smallest proportion of "very hot" areas (0.7%), followed by B2 (2.4%), B2 "hot" and "very hot" categories had the smallest sum of proportions, followed by B1, and B3 area was the largest, accounting for 81.2%; thus, B2 had a higher thermal comfort level at this time, followed by B1 and B4. The order of thermal comfort of different semi-open spaces was B2 > B1 > B4 > B3. In the semi-closed

space, the proportion of areas with a thermal comfort grade of "slightly warm" was 35.1% in C1, and 22.7% in C2, whereas the proportion of areas with a thermal comfort grade of "very hot" was 5.2% in C2 compared with 0% in C1. Therefore, the thermal comfort environment of C1 at 09:00 was superior to that of C2. In the fully closed space, there were four grades of thermal comfort, with a greater proportion of "very hot" sensation in D2 (48.4%) than in D1 (37.4%), and also a greater proportion of "slightly warm" sensation in D2 (28.9%) than D1 (6.8%) (Figure 18).

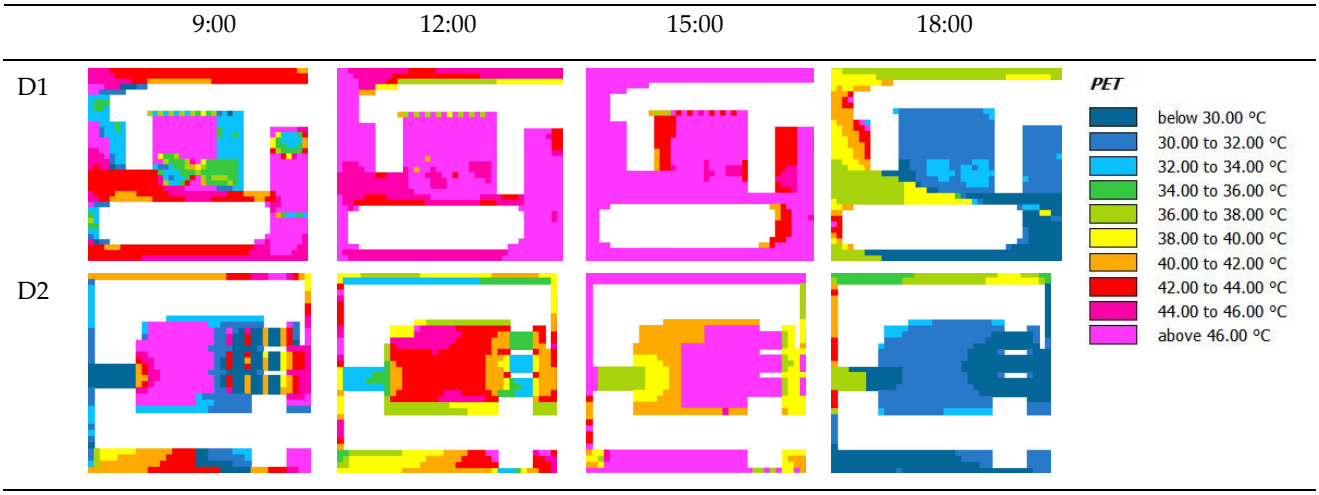

Figure 17. Spatiotemporal distribution of the PET in the fully enclosed space.

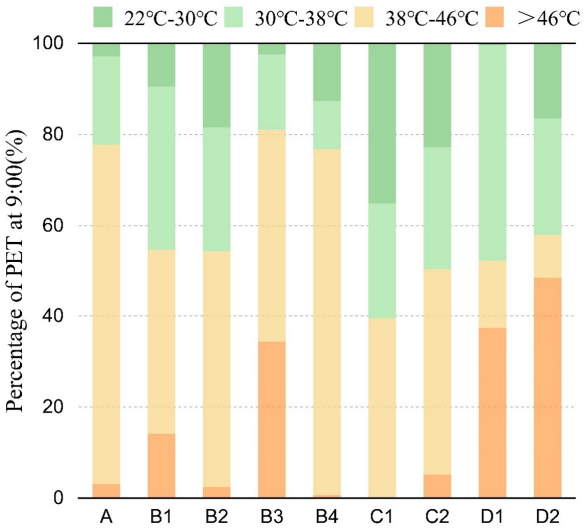

Figure 18. PET values of all levels of all spaces at 9:00.

3.4.3. Percentage of Thermal Comfort Grade at 12:00

At 12:00, 93.4% of the areas had a PET value within the range of 38–46 °C, also making the thermal sensation "hot" in fully open space. The PET values in all four semi-open areas were changed, and the thermal comfort changed to three grades. The proportion of "very hot" areas had expanded, with "very hot" areas accounting for the largest proportion in B3 (57.4), followed by B1 (43.4%). B4 had the largest proportion of "warm" areas (14.3%) and "very hot" areas accounted for the smallest proportion (0.4%). The order of thermal comfort in each area was B4 > B1 > B2 > B3. There were only two grades of thermal comfort, "warm" and "hot" in semi-closed spaces. The percentage of "warm" areas in C1 (19%) was higher than that of C2 (7.7%). The thermal comfort environment of C1 at 12:00 was better than that of C2. In fully closed spaces, the "very hot" area in D1 reached its maximum daily

value, accounting for ≤80.9% of the area, whereas the "very hot" area in D2 also expanded slightly (about 0.7%). The thermal comfort environment of D2 at 12:00 was better than that of D1(Figure 19).

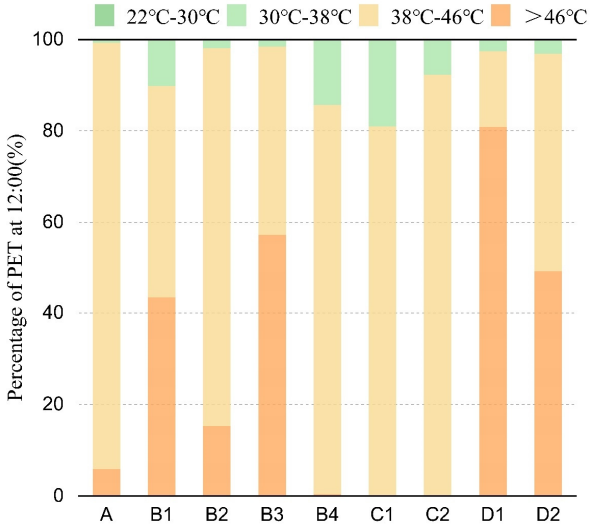

Figure 19. PET values of all levels of all spaces at 12:00.

3.4.4. Percentage of Thermal Comfort Grade at 15:00

At 15:00, the thermal comfort grade increased with higher temperatures and Tmrt, resulting in a higher percentage of "very hot" thermal sensations (80.4%), and thus creating a very poor thermal comfort environment in fully open space. In semi-open spaces, as the Ta gradually increased and the solar radiation strengthened, the PET value reached its peak, and the corresponding thermal comfort levels were at their worst. Among them, the proportion of "very hot" areas in the B4 area reached 80.5%, followed by B3 at 57.9%, and the sum of the proportions of "slightly warm" and "warm" areas in B1 was the highest (43.6%). Thus, at this time, the order of thermal comfort in each area was B1 > B2 > B3 > B4. The number of thermal comfort grades increased to three-"warm," "hot", and "very hot" in semi-closed spaces. Namely, the proportion of "very hot" (49.4%) areas in C2 was lower than that in C1 (53.2%). At the same time, the proportion of C1 "warm" (6.7%) areas was higher than that of C2 (1.7%). In fully closed spaces, the "very hot" area in D2 expanded slightly (1.2%), while the "very hot" area in D1 shrunk (2.5%). The thermal comfort environment of D2 at 15:00 was better than that of D1 and the overall uncomfortable area remained large (Figure 20).

3.4.5. Percentage of Thermal Comfort Grade at 18:00

At 18:00, "slightly warm" and "warm" accounted for a relatively large proportion of the study area, and the overall comfort was good in fully open space. In semi-open spaces, as the solar altitude angle became smaller, the Ta and solar radiation decreased, and the thermal environment of the campus became more comfortable, with the grades of PET values here shifting to "slightly warm," "warm", and "hot". Among them, B1 "slightly warm" areas accounted for the highest proportion (82%), followed by B3 (70.6%). The order of thermal comfort for each area at this time was B1 > B3 > B2 > B4. Among them, B1 "slightly warm" areas accounted for the highest proportion (82%), followed by B3 (70.6%). The thermal comfort environment of C2 was better than that of C1. In fully closed spaces, the thermal comfort grades in D1 were "slightly warm", "warm", and "hot", whereas those in D2 were only "slightly warm" and "warm". The percentage of "slightly warm" areas in D2 (28.9%) was higher than that in D1 (6.8%), and the percentage of "hot" grade in D1 was 5.4%. In summary, fully enclosed areas had a poor thermal comfort environment, and are less suitable for outdoor activities(Figure 21).

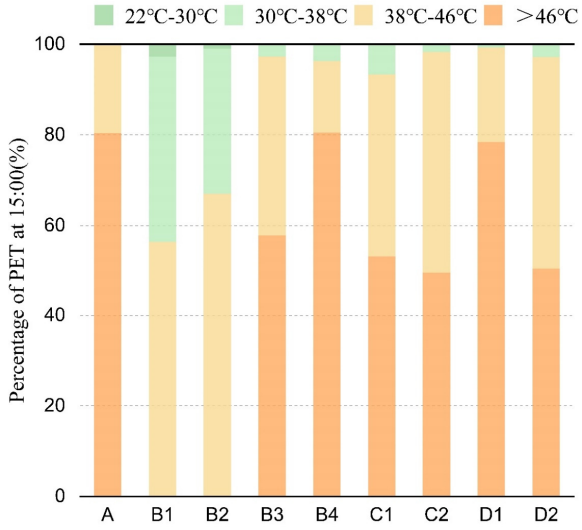

Figure 20. PET values of all levels of all spaces at 15:00.

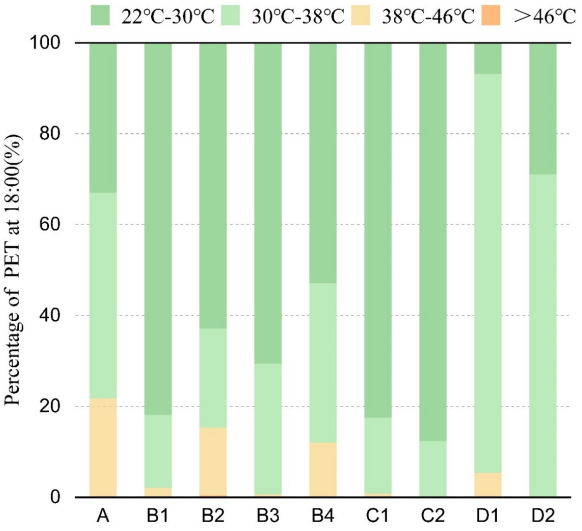

Figure 21. PET values of all levels of all spaces at 18:00.

3.5. Strategies for Improving Outdoor Spaces on Campus Based on Thermal Comfort

Traditional campus outdoor space design is mainly based on spatial aesthetics and functionality, often lacking consideration for the sustainability and climate adaptation of green campuses, which could easily lead to the deterioration of outdoor thermal comfort environments [63]. It has long been hoped to provide better outdoor thermal comfort conditions by changing the configuration of the environment, mainly including the establishment of green space, providing shading facilities, the cooling benefits of water bodies, cold underlying surface materials, etc. [5]. In terms of comprehensive thermal comfort levels, changing the urban geometry provides the greatest improvement, followed by vegetation, water bodies, and the cold surface [64]. Therefore, to improve the thermal comfort of campuses, rational planning and design of spatial forms and landscape elements based on climate adaptation are essential.

3.5.1. Experimental Design for Optimizing Outdoor Spaces

For the hot-summer and cold-winter zones, efforts should be made to improve outdoor comfort during these seasons (especially summer) [65]. Accordingly, the experimental optimization solution should focus on improving extremely hot conditions in the summer. Of the four study areas, the courtyard of the logistics building had the worst thermal comfort conditions in the summer among the fully enclosed spaces, and improving its

overall environment should be prioritized. Therefore, the courtyard of the logistics building (fully enclosed space) was selected as the experimental transformation area. Landscape elements were designed to intervene in the microclimate of the site, thus optimizing thermal comfort without changing the geometric structure of the building.

3.5.2. Optimization Scheme Design and Model Construction

From the previous analysis of the logistics building's courtyard, PET was lowest at 09:00 in the shadow of the buildings on the southwest side, and at 15:00 on the west side of the site and below the trees. The transformation strategy of a fully enclosed space mainly involves adding landscape structures to provide shade, enriching plant configuration, and improving the materials of the underlying surface. The activity areas were arranged in combination with buildings and trees. Hefei has a high Tmrt in summer, and a relatively poor thermal comfort environment; therefore, shading is required to create a more suitable comfort environment.

This design set up two leisure places: in the morning, the one on the southeast side could be used for activities, making full use of the shading effect of the vegetation itself. In the afternoon, a suitable thermal comfort environment was created by utilizing the shade of the building on the west side and arranging a veranda 2 m to its right to further expand the shaded area. The cooling and humidifying effect of plants can affect the internal microclimate of the courtyard to a certain extent; therefore, in summer, plants should be used to create shaded spaces, but trees with too low branching points could obstruct the ventilation at human height, and detrimentally affect OTC. Accordingly, existing *Cinnamomum camphora (Linn) Presl*, *Osmanthus fragrans (Thunb.) Lour*, and *Diospyros kaki Thunb* on the site were kept, and *Platanus acerifolia* (deciduous trees) were planted as supplements. The trees can not only create sufficient shading in summer to improve thermal comfort, but also increase the transmission of sunlight in winter, to prevent excessive sun blocking from reducing thermal comfort [38]. Meanwhile, the planting of shrubs and herbaceous plants was also increased to enrich plant types and levels, thereby constituting a rich enclosure to enhance cooling and humidifying effects [66]. Two plane trees were planted in the northwest and southeast corners of the courtyard, and the existing trees on the site were transplanted. Owing to poor ventilation in the enclosed courtyard, the *Cinnamomum camphora (Linn) Presl* was transplanted to a ventilated place on the southwest side of the courtyard, thus changing the wind direction and increasing the air circulation inside the site. The original granite paving was also replaced by permeable concrete. Granite paving has high reflectance, and some scholars maintain that high reflectance increases the short-wave radiation, and Tmrt of the pavement [67], thereby creating an uncomfortable thermal environment. In contrast, permeable materials can store rainwater because of their large pores, and cool the surface temperature through evaporation, which can improve thermal comfort to a certain extent. Additionally, permeable paving can recharge groundwater, reduce surface runoff, and absorb noise.

After several rounds of design and simulation comparisons of the transformation plan, the results post-transformation results are shown in Figure 22. Areas 1 and 3 were the activity locations. Located along the roadside, Area 1 was more open and can be used as a space for club activities, whereas Area 3 was a more private space for teachers and students to read and communicate outdoors.

3.5.3. Percentage of Each Thermal Comfort Grade

The modified scheme was simulated, and the size, accuracy, and meteorological data of the modeling courtyard were consistent with those of the original scheme. Microclimate simulations were performed for the optimized scheme, and the spatiotemporal distribution graphs of PET at 09:00, 12:00, 15:00, and 18:00 were generated, and then compared with the PET distribution graphs before the transformation. The PET differences and mean temperature changes in the courtyard pre- and post-transformation were calculated (Figure 23).

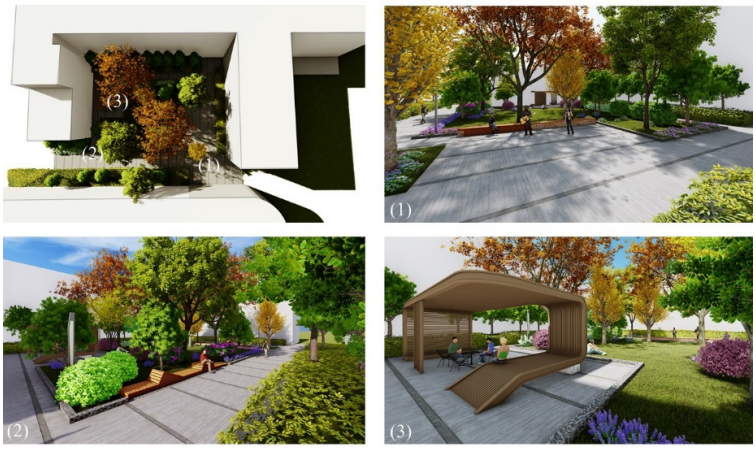

Figure 22. Modified renderings. (1) is the plan of simulation renovation, and (2)–(4) are the effect drawing of the corresponding position in the plan.

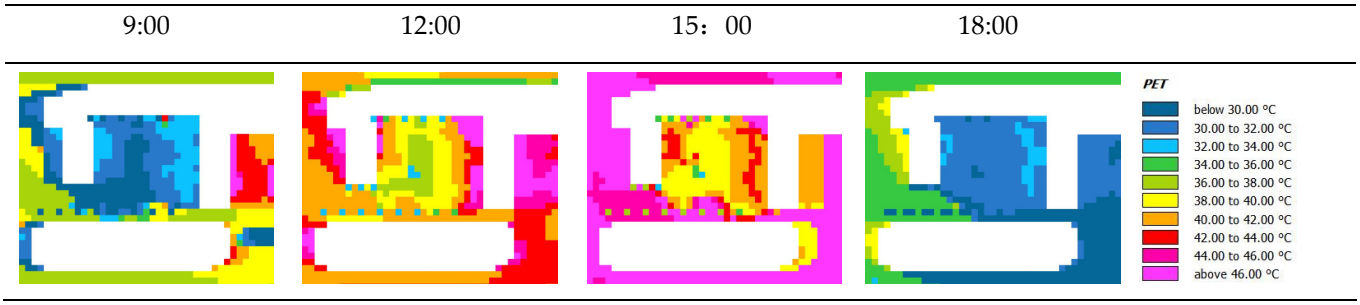

Figure 23. Distribution and variation of the PET values of the modification scheme.

The distribution of PET values before and after the renovation is compared in Figure 24. At 9:00, the PET value in most areas of the courtyard was blue, PET was below 30 °C, and the thermal comfort was "slightly warm" and "warm", of which the proportion of "slightly warm" areas changed from the original 0.4% to 29%. Further, the proportion of "warm" areas increased from 47.1% to 68%, the proportion of "hot" areas decreased from 15.1% to 3%, and the area after renovation had no "very hot" areas at 9:00. The largest decrease in PET values in the middle and northwest areas of the site was mainly due to the addition of shading facilities here, and the larger canopy of the plants, which provided more shade space, and had the overall effect of lowering the Ta.

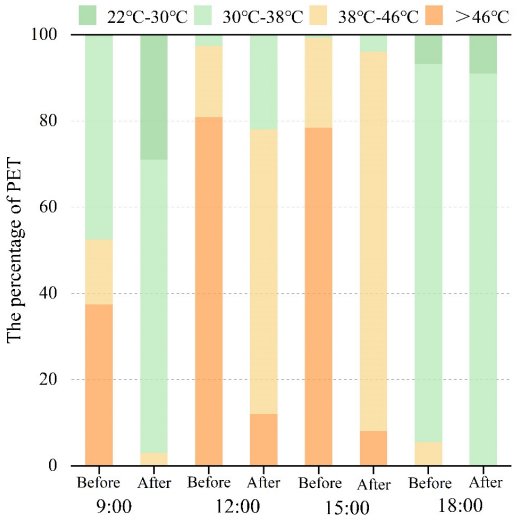

Figure 24. The PET value changes at each moment before and after the modification.

At 12:00, the overall PET of the courtyard increased, 66 % of the area reached the "hot" category, 12% of the area had a temperature >46 °C, and the thermal feeling was "very hot", compared with the "hot" range of 16.5% and the "very hot" range of 80.9%; in the front courtyard before the renovation, the overall PET decreased and the thermal comfort improved.

At 15:00, the PET value in most areas of the courtyard was below 46 °C, and the range of the "very hot" category had reduced from 78.4% to 8% compared to that at 12:00, and the effect of the renovation was distinct.

At 18:00, the thermal comfort level of the courtyard was generally good, most of the PET values in the site were between 30–38 °C, the thermal feeling was "warm", and the thermal comfort level before the renovation was similar. Further, the PET value under the tree increased slightly, because the effective long-wave radiation emitted under the canopy was slow and the heat was not getting easily dissipated. Although the effect of changing PET value at 18:00 was not as significant as that compared with other times, the effect of transformation in the hot period of the day was distinct, which suggests the feasibility of this scheme.

4. Discussion

A comparative analysis of the thermal comfort of different outdoor space forms showed that the correlation between the Tmrt and thermal comfort was high [68–70]. The Tmrt in the shadows of trees and buildings was low, and the corresponding PET value was relatively low as well. In particular, there are lawns or shrubs under the trees which can cool and humidify the micro-climate; moreover, the long-wave radiation is weak, and the resulting PET value is the lowest. The PET values were also lower for trees with larger crowns *(Koelreuteria paniculata*). Additionally, there was a significant negative correlation between Ws and PET [71]. With the same Tmrt, the Ws at the corner of the building was higher, and the PET value was lower, whereas the Ws at the east and west sides of the building were lower, and the resulting PET value was higher. Although the improvement effect of small water bodies on the thermal comfort of the surrounding environment was weak, appropriately expanding the shaded area, building sunshade components, and increasing the coverage of campus plants can effectively improve the thermal comfort of this space in summer. The material of the underlying surface also affects thermal comfort. As ground surfaces reflect solar radiation or heat the air above them, pavements that can absorb more solar radiation may become a radiating body, thus warming the surrounding air, heating urban areas, and decreasing the thermal comfort for people [72].

The thermal comfort environment of each space was the worst at 15:00 and the best at 18:00 due to the solar altitude angle and solar radiation. Among them, in the semi-open space, the PET value of 9:00 in B2 was the best, mainly because the building is on the east side of the site, the sun shines in from the east, and the shadow area formed by the building is relatively large. The PET value of B4 was the best at 12:00, and at 15:00, and 18:00 in the afternoon, and the PET value in B1 was the best, mainly because the bottom floor of some buildings in the B1 area is elevated, the wind environment is better, and the B1 area is built on the west side of the site. Further, B1 is affected by the sun height angle, the shadow range formed by the building is larger, and the B1 area has a larger arbor crown. Therefore, the overall thermal comfort of the B1 area in the afternoon was better. In the semi-enclosed space, the thermal comfort of C1 at 9:00 and 12:00 was better than that of C2. The thermal comfort of C2 in the afternoon is better than that of C1, mainly because the position of the building's shadow changes as the height angle of the sun changes. The thermal comfort environment of the fully enclosed space was poor, the "very hot" category range was large, and the duration was long. The thermal comfort environment of the D1 courtyard was generally inferior to that of the D2 courtyard, and the area with a thermal feeling of the "very hot" category accounted for a large proportion. Based on a comprehensive analysis of the thermal comfort of these four types of spaces on campus in a day, it was found that the thermal comfort of the fully enclosed space was the worst, followed by the low thermal

comfort of the fully open space. The thermal comfort environment of the semi-enclosed space was the best, followed by the half-open space.

The simulation results suggest that the thermal comfort of the fully enclosed space (D1) with the worst thermal comfort can be improved by adding shading structures (summerhouse), enriching plant configurations, and changing the underlying material without modifying the building. By comparing the PET value before and after the transformation at the same time of the day, it can be seen that the PET value after the transformation had decreased, and the thermal comfort had significantly improved. The shading structure can effectively block solar radiation and have a significant cooling effect in summer [73]. Effective tree placement and arrangement can improve outdoor microclimate and thermal comfort. Plant levels and species should be enriched and placed in groups and overlapping canopies should be avoided when designing to provide more shade, and the introduction of vegetation has an overall cooling effect. Through the survey of thermal comfort, it can be seen that pedestrians prefer grass in hot summer [74]. Therefore, expanding the area of grass cover is an effective strategy to improve PET. At the same time, permeable concrete can increase pavement evaporation, reduce pavement temperature, and improve thermal comfort to a certain extent. Therefore, through the simulated transformation, it can be seen that in the hot summer, providing shade structures, increasing the planting of trees, especially trees with larger canopies, and improving the underlying surface material has a significant effect on thermal comfort.

5. Conclusions

In this study, the southern campus of AHJZU was selected as the research area. The 29 April and 13 November were selected as the monitoring dates for field measurements to verify the applicability of the ENVI-met within the Hefei area. During a typical summer climate, four outdoor space types were selected for thermal comfort research. Here, the PET thermal comfort index was calculated, revealing that the fully enclosed space produced the worst thermal comfort. Thus, this space was simulated and transformed, and the modified PET thermal comfort index was calculated. The main conclusions of this study are as follows:

(1) The field measurement data were compared with the ENVI-met simulation data to obtain the temperature, RMS coefficient, RMS error, and consistency index for each measured point. The results supported that the temperature, RMS error, and wind speed index of each measurement point were within the error range, indicating that ENVI-met well represented the changing trends, and supporting its applicability within the Hefei area. The consistency index of the summer meteorological parameters was close to 1, indicating that the ENVI-met performed better in the summer than in winter.

(2) Owing to the various architectural modes and plant configurations, the spatial and temporal distributions of PET were quite different. A comprehensive analysis of the thermal comfort of these four types of spaces in the campus showed that the thermal comfort of the fully enclosed space was the worst, followed by the poor fully open space. Comparatively, the thermal comfort environment of the semi-enclosed space was the best, followed by the semi-open space. Therefore, in the planning and construction of the campus, the spatial form of semi-enclosed space (U-shaped) is preferred. This may be mainly because the U-shaped surrounding buildings better block solar radiation and provide more shade. At the same time, both C1 and C2 are semi-enclosed spaces, but the thermal comfort level of C1 is generally better than that of C2, mainly because C1 has more abundant plant groups and a high proportion of permeable underwater cushion surfaces, which can improve thermal comfort. Through the classification and analysis of different outdoor spaces, the differences in thermal comfort and thermal comfort levels at different time points were obtained to propose suggestions and references for the optimization of outdoor campus environments.

A comparative analysis of the thermal comfort of different outdoor space forms showed that the correlation between the Tmrt and thermal comfort was high [68–70]. The Tmrt in the shadows of trees and buildings was low, and the corresponding PET value was

relatively low as well. In particular, there are lawns or shrubs under the trees which can cool and humidify the micro-climate; moreover, the long-wave radiation is weak, and the resulting PET value is the lowest. The PET values were also lower for trees with larger crowns *(Koelreuteria paniculata*). Additionally, there was a significant negative correlation between Ws and PET [71]. With the same Tmrt, the Ws at the corner of the building was higher, and the PET value was lower, whereas the Ws at the east and west sides of the building were lower, and the resulting PET value was higher. Although the improvement effect of small water bodies on the thermal comfort of the surrounding environment was weak, appropriately expanding the shaded area, building sunshade components, and increasing the coverage of campus plants can effectively improve the thermal comfort of this space in summer. The material of the underlying surface also affects thermal comfort. As ground surfaces reflect solar radiation or heat the air above them, pavements that can absorb more solar radiation may become a radiating body, thus warming the surrounding air, heating urban areas, and decreasing the thermal comfort for people [72].

(3) To address the thermal comfort of the worst fully enclosed space, a simulation was run by increasing landscape structures to provide shade spaces and rich plant configurations. Accordingly, the PET spatiotemporal distribution compared with before showed varying levels of improvement, especially during the day when the effects were more obvious.

In conclusion, this research showed that the thermal comfort of university campuses is influenced by the building mode, plant configuration, and underlying surface materials. The findings here can provide theoretical support and serve as a technical reference for the construction of a more thermally comfortable university campus. The study yielded satisfactory results, but some limitations remained. Firstly, it should be pointed out that based on the typical summer weather in June, there is a lack of research on the transition seasons. Secondly, longer measurement times are needed to collect a more comprehensive and convincing database. Finally, the relevant content of the questionnaire survey should be supplemented in the study to better explore the impact of different landscape elements and layouts on human thermal comfort. In follow-up research, the seasons and their duration will be expanded to explore and analyze the impacts of the dynamic changes of different weather conditions on the thermal comfort of campus outdoor spaces.

Author Contributions: Conceptualization, S.Z., S.L., L.S., T.X. and T.S.; methodology, S.L. and L.S.; software, S.L. and L.S.; validation, S.Z., T.X. and S.L.; formal analysis, S.Z., S.L., T.X., L.S. and T.S.; data curation, S.Z., T.X. and T.S.; writing—original draft preparation, S.Z., S.L., L.S., T.X. and T.S.; writing—review and editing, S.Z., T.X. and S.L.; visualization, L.S.; supervision, S.Z. and T.X.; funding acquisition, T.X. and T.S. All authors have read and agreed to the published version of the manuscript.

Funding: This research was funded by the National Natural Science Foundation of China Youth Project "Development of a dynamic model for predicting wind and thermal environment in hot summer and cold winter cities considering the spatial heterogeneity of urban surfaces", grant number 52008001; Anhui Provincial Department of Education Major Project "Research on the Path and Strategy of Rural Development at the County under the Dual Guidance of Land Spatial Planning and Rural Revitalization Strategy—Taking Lujiang County, Hefei City as an Example", grant number SK2020ZD25; Natural Science Foundation of the Anhui Higher Education Institutions of China "Non-steady-state prediction model of thermal climate in urban residential areas in hot summer and cold winter", grant number KJ2019A0762; and Anhui Province prefabricated building research institutions scientific research platform open project "Research on carbon emissions of prefabricated garden buildings under the background of double carbon", grant number AHZPY2021ZR02; Anhui University Scientific Research Project in 2022 "Research on the emotional design of urban public green space based on multimodal data—Taking the main urban area of Hefei as an example", grant number 2022AH050226.

Institutional Review Board Statement: Not applicable.

Informed Consent Statement: Not applicable.

Data Availability Statement: Publicly available datasets were analyzed in this study. These data can be found on the campus IoT weather station.

Conflicts of Interest: The authors declare no conflict of interest.

References

1. Cao, Q.; Yu, D.Y.; Georgescu, M.; Wu, J.G.; Wang, W. Impacts of future urban expansion on summer climate and heat-related human health in eastern China. *Environ. Int.* **2018**, *112*, 134–146. [CrossRef] [PubMed]
2. Deilami, K.; Kamruzzaman, M.; Liu, Y. Urban heat island effect: A systematic review of spatio-temporal factors, data, methods, and mitigation measures. *Int. J. Appl. Earth Obs.* **2018**, *67*, 30–42. [CrossRef]
3. Santamouris, M. On the energy impact of urban heat island and global warming on buildings. *Energy Build.* **2014**, *82*, 100–113. [CrossRef]
4. Lee, Y.Y.; Din, M.F.M.; Ponraj, M.; Noor, Z.Z.; Iwao, K.; Chelliapan, S. Overview of Urban Heat Island (Uhi) Phenomenon towards Human Thermal Comfort. *Environ. Eng. Manag. J.* **2017**, *16*, 2097–2111.
5. Lai, D.Y.; Liu, W.Y.; Gan, T.T.; Liu, K.X.; Chen, Q.Y. A review of mitigating strategies to improve the thermal environment and thermal comfort in urban outdoor spaces. *Sci. Total Environ.* **2019**, *661*, 337–353. [CrossRef] [PubMed]
6. Cao, W.J.; Fang, Z.W.; Hou, G.Q.; Han, M.; Xu, X.R.; Dong, J.X.; Zheng, J.Z. The psychological impact of the COVID-19 epidemic on college students in China. *Psychiat. Res.* **2020**, *287*, 112934. [CrossRef]
7. Liu, S.B.; Ji, Y.F.; Li, J.; Peng, Y.; Li, Z.T.; Lai, W.B.; Feng, T. Analysis of students' positive emotions around the green space in the university campus during the COVID-19 pandemic in China. *Front. Public Health* **2022**, *10*, 888295. [CrossRef]
8. Liu, L.; Liang, Z.X.; Liu, J.; Du, J.; Zhang, H.B. Field Survey on Local Thermal Comfort of Students at a University Campus: A Case Study in Shanghai. *Atmosphere* **2022**, *13*, 1433. [CrossRef]
9. Sun, B.; Zhang, H.; Zhao, L.; Qu, K.C.; Liu, W.H.; Zhuang, Z.C.; Ye, H.Y. Microclimate Optimization of School Campus Landscape Based on Comfort Assessment. *Buildings* **2022**, *12*, 1375. [CrossRef]
10. Kumar, P.; Sharma, A. Study on importance, procedure, and scope of outdoor thermal comfort—A review. *Sustain. Cities Soc.* **2020**, *61*, 102297. [CrossRef]
11. Hong, B.; Lin, B.R. Numerical study of the influences of different patterns of the building and green space on micro-scale outdoor thermal comfort and indoor natural ventilation. *Build. Simul.* **2014**, *7*, 525–536. [CrossRef]
12. Hong, B.; Lin, B.R. Numerical studies of the outdoor wind environment and thermal comfort at pedestrian level in housing blocks with different building layout patterns and trees arrangement. *Renew. Energy* **2015**, *73*, 18–27. [CrossRef]
13. Su, Y.; Zhao, Q.F.; Zhou, N. Improvement strategies for thermal comfort of a city block based on PET Simulation—A case study of Dalian, a cold-region city in China. *Energy Build.* **2022**, *261*, 111557. [CrossRef]
14. Rui, L.Y.; Buccolieri, R.; Gao, Z.; Gatto, E.; Ding, W.W. Study of the effect of green quantity and structure on thermal comfort and air quality in an urban-like residential district by ENVI-met modelling. *Build. Simul.* **2019**, *12*, 183–194. [CrossRef]
15. Sayad, B.; Alkama, D.; Rebhi, R.; Menni, Y.; Ahmad, H.; Inc, M.; Sharifpur, M.; Lorenzini, G.; Azab, E.; Elnaggar, A.Y. Outdoor Thermal Comfort Optimization through Vegetation Parameterization: Species and Tree Layout. *Sustainability* **2021**, *13*, 11791. [CrossRef]
16. Zhao, Q.S.; Sailor, D.J.; Wentz, E.A. Impact of tree locations and arrangements on outdoor microclimates and human thermal comfort in an urban residential environment. *Urban Urban Green.* **2018**, *32*, 81–91. [CrossRef]
17. Zheng, B.H.; Bedra, K.B.; Zheng, J.; Wang, G.G. Combination of Tree Configuration with Street Configuration for Thermal Comfort Optimization under Extreme Summer Conditions in the Urban Center of Shantou City, China. *Sustainability* **2018**, *10*, 4192. [CrossRef]
18. Aboelata, A. Reducing outdoor air temperature, improving thermal comfort, and saving buildings' cooling energy demand in arid cities—Cool paving utilization. *Sustain. Cities Soc.* **2021**, *68*, 102762. [CrossRef]
19. Djekic, J.; Djukic, A.; Vukmirovic, M.; Djekic, P.; Brankovic, M.D. Thermal comfort of pedestrian spaces and the influence of pavement materials on warming up during summer. *Energy Build.* **2018**, *159*, 474–485. [CrossRef]
20. Din, M.F.M.; Lee, Y.Y.; Ponraj, M.; Ossen, D.R.; Iwao, K.; Chelliapan, S. Thermal comfort of various building layouts with a proposed discomfort index range for tropical climate. *J. Therm. Biol.* **2014**, *41*, 6–15. [CrossRef]
21. Taleghani, M.; Tenpierik, M.; van den Dobbelsteen, A.; Sailor, D.J. Heat in courtyards: A validated and calibrated parametric study of heat mitigation strategies for urban courtyards in the Netherlands. *Sol. Energy* **2014**, *103*, 108–124. [CrossRef]
22. Afshar, N.K.; Karimian, Z.; Doostan, R.; Nokhandan, M.H. Influence of Planting Designs on Winter Thermal Comfort in an Urban Park. *J. Environ. Eng. Landsc.* **2018**, *26*, 232–240. [CrossRef]
23. Milosevic, D.D.; Bajsanski, I.V.; Savic, S.M. Influence of changing trees locations on thermal comfort on street parking lot and footways. *Urban Urban Green.* **2017**, *23*, 113–124. [CrossRef]
24. Morakinyo, T.E.; Dahanayake, K.W.D.K.C.; Adegun, O.B.; Balogun, A.A. Modelling the effect of tree-shading on summer indoor and outdoor thermal condition of two similar buildings in a Nigerian university. *Energy Build.* **2016**, *130*, 721–732. [CrossRef]
25. Altunkasa, C.; Uslu, C. Use of outdoor microclimate simulation maps for a planting design to improve thermal comfort. *Sustain. Cities Soc.* **2020**, *57*, 102137. [CrossRef]
26. Taleghani, M. The impact of increasing urban surface albedo on outdoor summer thermal comfort within a university campus. *Urban Clim.* **2018**, *24*, 175–184. [CrossRef]
27. Cortesao, J.; Alves, F.B.; Corvacho, H.; Rocha, C. Retrofitting public spaces for thermal comfort and sustainability. *Indoor Built Environ.* **2016**, *25*, 1085–1095.

28. Wang, J.S.; Meng, Q.L.; Tan, K.H.; Zhang, L.; Zhang, Y. Experimental investigation on the influence of evaporative cooling of permeable pavements on outdoor thermal environment. *Build. Environ.* **2018**, *140*, 184–193. [CrossRef]
29. Antoniadis, D.; Katsoulas, N.; Papanastasiou, D.; Christidou, V.; Kittas, C. Evaluation of thermal perception in schoolyards under Mediterranean climate conditions. *Int. J. Biometeorol.* **2016**, *60*, 319–334. [CrossRef]
30. Ghaffarianhoseini, A.; Berardi, U.; Ghaffarianhoseini, A.; Al-Obaidi, K. Analyzing the thermal comfort conditions of outdoor spaces in a university campus in Kuala Lumpur, Malaysia. *Sci. Total Environ.* **2019**, *666*, 1327–1345. [CrossRef]
31. Antoniadis, D.; Katsoulas, N.; Papanastasiou, D.K. Thermal Environment of Urban Schoolyards: Current and Future Design with Respect to Children's Thermal Comfort. *Atmosphere* **2020**, *11*, 1144. [CrossRef]
32. Zaki, S.A.; Syahidah, S.W.; Shahidan, M.F.; Ahmad, M.I.; Yakub, F.; Hassan, M.Z.; Daud, M.Y.M. Assessment of Outdoor Air Temperature with Different Shaded Area within an Urban University Campus in Hot-Humid Climate. *Sustainability* **2020**, *12*, 5741. [CrossRef]
33. Wu, Z.F.; Chen, L.D. Optimizing the spatial arrangement of trees in residential neighborhoods for better cooling effects: Integrating modeling with in-situ measurements. *Landsc. Urban Plan* **2017**, *167*, 463–472. [CrossRef]
34. Lin, T.P.; Matzarakis, A.; Hwang, R.L. Shading effect on long-term outdoor thermal comfort. *Build. Environ.* **2010**, *45*, 213–221. [CrossRef]
35. Zhang, A.X.; Bokel, R.; van den Dobbelsteen, A.; Sun, Y.C.; Huang, Q.; Zhang, Q. An integrated school and schoolyard design method for summer thermal comfort and energy efficiency in Northern China. *Build. Environ.* **2017**, *124*, 369–387. [CrossRef]
36. Gao, Y.F.; Yao, R.M.; Li, B.Z.; Turkbeyler, E.; Luo, Q.; Short, A. Field studies on the effect of built forms on urban wind environments. *Renew. Energy* **2012**, *46*, 148–154. [CrossRef]
37. Xu, M.; Hong, B.; Mi, J.Y.; Yan, S.S. Outdoor thermal comfort in an urban park during winter in cold regions of China. *Sustain. Cities Soc.* **2018**, *43*, 208–220. [CrossRef]
38. Zheng, S.L.; Zhao, L.H.; Li, Q. Numerical simulation of the impact of different vegetation species on the outdoor thermal environment. *Urban Urban Green.* **2016**, *18*, 138–150. [CrossRef]
39. Yang, J.Y.; Hu, X.Y.; Feng, H.Y.; Marvin, S. Verifying an ENVI-met simulation of the thermal environment of Yanzhong Square Park in Shanghai. *Urban Urban Green.* **2021**, *66*, 127384. [CrossRef]
40. Tsoka, S.; Tsikaloudaki, A.; Theodosiou, T. Analyzing the ENVI-met microclimate model's performance and assessing cool materials and urban vegetation applications—A review. *Sustain. Cities Soc.* **2018**, *43*, 55–76. [CrossRef]
41. Sun, S.B.; Xu, X.Y.; Lao, Z.M.; Liu, W.; Li, Z.D.; Garcia, E.H.; He, L.; Zhu, J.N. Evaluating the impact of urban green space and landscape design parameters on thermal comfort in hot summer by numerical simulation. *Build. Environ.* **2017**, *123*, 277–288. [CrossRef]
42. Mahmoud, R.M.A.; Abdallah, A.S.H. Assessment of outdoor shading strategies to improve outdoor thermal comfort in school courtyards in hot and arid climates. *Sustain. Cities Soc.* **2022**, *86*, 104147. [CrossRef]
43. Rui, L.Y.; Buccolieri, R.; Gao, Z.; Ding, W.W.; Shen, J.L. The Impact of Green Space Layouts on Microclimate and Air Quality in Residential Districts of Nanjing, China. *Forests* **2018**, *9*, 224. [CrossRef]
44. Yang, Y.J.; Zhou, D.; Wang, Y.P.; Ma, D.X.; Chen, W.; Xu, D.; Zhu, Z.Z. Economical and outdoor thermal comfort analysis of greening in multistory residential areas in Xi'an. *Sustain. Cities Soc.* **2019**, *51*, 101730. [CrossRef]
45. Yang, W.; Wong, N.H.; Li, C.Q. Effect of Street Design on Outdoor Thermal Comfort in an Urban Street in Singapore. *J. Urban Plan. Dev.* **2016**, *142*, 05015003. [CrossRef]
46. Narimani, N.; Karimi, A.; Brown, R.D. Effects of street orientation and tree species thermal comfort within urban canyons in a hot, dry climate. *Ecol. Inform.* **2022**, *69*, 101671. [CrossRef]
47. Karimi, A.; Sanaieian, H.; Farhadi, H.; Norouzian-Maleki, S. Evaluation of the thermal indices and thermal comfort improvement by different vegetation species and materials in a medium-sized urban park. *Energy Rep.* **2020**, *6*, 1670–1684. [CrossRef]
48. Chan, S.Y.; Chau, C.K. On the study of the effects of microclimate and park and surrounding building configuration on thermal comfort in urban parks. *Sustain. Cities Soc.* **2021**, *64*, 102512. [CrossRef]
49. Sayad, B.; Alkama, D.; Ahmad, H.; Baili, J.; Aljahdaly, N.H.; Menni, Y. Nature-based solutions to improve the summer thermal comfort outdoors. *Case Stud. Therm. Eng.* **2021**, *28*, 101399. [CrossRef]
50. Lam, C.K.C.; Lee, H.; Yang, S.R.; Park, S. A review on the significance and perspective of the numerical simulations of outdoor thermal environment. *Sustain. Cities Soc.* **2021**, *71*, 102971. [CrossRef]
51. Muller, N.; Kuttler, W.; Barlag, A.B. Counteracting urban climate change: Adaptation measures and their effect on thermal comfort. *Theor. Appl. Climatol.* **2014**, *115*, 243–257. [CrossRef]
52. Farhadi, H.; Faizi, M.; Sanaieian, H. Mitigating the urban heat island in a residential area in Tehran: Investigating the role of vegetation, materials, and orientation of buildings. *Sustain. Cities Soc.* **2019**, *46*, 101448. [CrossRef]
53. Salata, F.; Golasi, L.; Vollaro, R.D.; Vollaro, A.D. Urban microclimate and outdoor thermal comfort. A proper procedure to fit ENVI-met simulation outputs to experimental data. *Sustain. Cities Soc.* **2016**, *26*, 318–343. [CrossRef]
54. Bande, L.; Afshari, A.; Al Masri, D.; Jha, M.; Norford, L.; Tsoupos, A.; Marpu, P.; Pasha, Y.; Armstrong, P. Validation of UWG and ENVI-Met Models in an Abu Dhabi District, Based on Site Measurements. *Sustainability* **2019**, *11*, 4378. [CrossRef]
55. Abd Elraouf, R.; ELMokadem, A.; Megahed, N.; Eleinen, O.A.; Eltarabily, S. Evaluating urban outdoor thermal comfort: A validation of ENVI-met simulation through field measurement. *J. Build. Perform. Simul.* **2022**, *15*, 268–286. [CrossRef]

56. Kim, S.W.; Brown, R.D. Pedestrians' behavior based on outdoor thermal comfort and micro-scale thermal environments, Austin, TX. *Sci. Total Environ.* **2022**, *808*, 152143. [CrossRef] [PubMed]
57. Stewart, I.D.; Oke, T.R. Local Climate Zones for Urban Temperature Studies. *Bull. Am. Meteorol. Soc.* **2012**, *93*, 1879–1900. [CrossRef]
58. Huang, Z.F.; Cheng, B.; Gou, Z.H.; Zhang, F. Outdoor thermal comfort and adaptive behaviors in a university campus in China's hot summer-cold winter climate region. *Build. Environ.* **2019**, *165*, 106414. [CrossRef]
59. Ma, D.; Wang, Y.; Zhou, D.; Zhu, Z. Cooling effect of the pocket park in the built-up block of a city: A case study in Xi'an, China. *Environ. Sci. Pollut. Res. Int.* **2022**. [CrossRef]
60. Potchter, O.; Cohen, P.; Lin, T.P.; Matzarakis, A. Outdoor human thermal perception in various climates: A comprehensive review of approaches, methods and quantification. *Sci. Total Environ.* **2018**, *631–632*, 390–406. [CrossRef]
61. Lai, D.Y.; Guo, D.H.; Hou, Y.F.; Lin, C.Y.; Chen, Q.Y. Studies of outdoor thermal comfort in northern China. *Build. Environ.* **2014**, *77*, 110–118. [CrossRef]
62. Liu, W.W.; Zhang, Y.X.; Deng, Q.H. The effects of urban microclimate on outdoor thermal sensation and neutral temperature in hot-summer and cold-winter climate. *Energy Build.* **2016**, *128*, 190–197. [CrossRef]
63. Hwang, R.L.; Weng, Y.T.; Huang, K.T. Considering transient UTCI and thermal discomfort footprint simultaneously to develop dynamic thermal comfort models for pedestrians in a hot-and-humid climate. *Build. Environ.* **2022**, *222*, 109410. [CrossRef]
64. Shooshtarian, S.; Rajagopalan, P.; Sagoo, A. A comprehensive review of thermal adaptive strategies in outdoor spaces. *Sustain. Cities Soc.* **2018**, *41*, 647–665. [CrossRef]
65. Qi, J.J.; Wang, J.P.; Zhai, W.Y.; Wang, J.Y.; Jin, Z.L. Are There Differences in Thermal Comfort Perception of Children in Comparison to Their Caregivers' Judgments? A Study on the Playgrounds of Parks in China's Hot Summer and Cold Winter Region. *Sustainability* **2022**, *14*, 10926. [CrossRef]
66. Bao, Y.; Gao, M.; Luo, D.; Zhou, X.D. The Influence of Plant Community Characteristics in Urban Parks on the Microclimate. *Forests* **2022**, *13*, 1342. [CrossRef]
67. Faragallah, R.N.; Ragheb, R.A. Evaluation of thermal comfort and urban heat island through cool paving materials using ENVI-Met. *Ain Shams Eng. J.* **2022**, *13*, 101609. [CrossRef]
68. Dissegna, M.A.; Yin, T.G.; Wu, H.; Lauret, N.; Wei, S.S.; Gastellu-Etchegorry, J.P.; Gret-Regamey, A. Modeling Mean Radiant Temperature Distribution in Urban Landscapes Using DART. *Remote Sens.* **2021**, *13*, 1443. [CrossRef]
69. Nazarian, N.; Fan, J.P.; Sin, T.; Norford, L.; Kleissl, J. Predicting outdoor thermal comfort in urban environments: A 3D numerical model for standard effective temperature. *Urban Clim.* **2017**, *20*, 251–267. [CrossRef]
70. Lau, K.K.L.; Ren, C.; Ho, J.; Ng, E. Numerical modelling of mean radiant temperature in high-density sub-tropical urban environment. *Energy Build.* **2016**, *114*, 80–86. [CrossRef]
71. Kang, K.N.; Song, D.; Schiavon, S. Correlations in thermal comfort and natural wind. *J. Therm. Biol.* **2013**, *38*, 419–426. [CrossRef]
72. Irmak, M.A.; Yilmaz, S.; Dursun, D. Effect of different pavements on human thermal comfort conditions. *Atmosfera* **2017**, *30*, 355–366. [CrossRef]
73. Watanabe, S.; Nagano, K.; Ishii, J.; Horikoshi, T. Evaluation of outdoor thermal comfort in sunlight, building shade, and pergola shade during summer in a humid subtropical region. *Build. Environ.* **2014**, *82*, 556–565. [CrossRef]
74. Rosso, F.; Pisello, A.L.; Cotana, F.; Ferrero, M. On the thermal and visual pedestrians' perception about cool natural stones for urban paving: A field survey in summer conditions. *Build. Environ.* **2016**, *107*, 198–214. [CrossRef]